

# Constrained SUSY seesaws with a 125 GeV Higgs

---

M. Hirsch<sup>a</sup> F. R. Joaquim<sup>b</sup> A. Vicente<sup>c</sup>

<sup>a</sup>*AHEP Group, Instituto de Física Corpuscular – C.S.I.C./Universitat de València, Edificio de Institutos de Paterna, Apartado 22085, E-46071 València, Spain*

<sup>b</sup>*Departamento de Física and Centro de Física Teórica de Partículas, Instituto Superior Técnico, Universidade Técnica de Lisboa, Av. Rovisco Pais, 1049-001 Lisboa, Portugal*

<sup>c</sup>*Laboratoire de Physique Théorique, CNRS – UMR 8627, Université de Paris-Sud 11, F-91405 Orsay Cedex, France*

*E-mail:* [mahirsch@ific.uv.es](mailto:mahirsch@ific.uv.es), [filipe.joaquim@ist.utl.pt](mailto:filipe.joaquim@ist.utl.pt),  
[avelino.vicente@th.u-psud.fr](mailto:avelino.vicente@th.u-psud.fr)

**ABSTRACT:** Motivated by the ATLAS and CMS discovery of a Higgs-like boson with a mass around 125 GeV, and by the need of explaining neutrino masses, we analyse the three canonical SUSY versions of the seesaw mechanism (type I, II and III) with CMSSM boundary conditions. In type II and III cases, SUSY particles are lighter than in the CMSSM (or the constrained type I seesaw), for the same set of input parameters at the universality scale. Thus, to explain  $m_{h^0} \simeq 125$  GeV at low energies, one is forced into regions of parameter space with very large values of  $m_0$ ,  $M_{1/2}$  or  $A_0$ . We compare the squark and gluino masses allowed by the ATLAS and CMS ranges for  $m_{h^0}$  (extracted from the 2011-2012 data), and discuss the possibility of distinguishing seesaw models in view of future results on SUSY searches. In particular, we briefly comment on the discovery potential of LHC upgrades, for squark/gluino mass ranges required by present Higgs mass constraints. A discrimination between different seesaw models cannot rely on the Higgs mass data alone, therefore we also take into account the MEG upper limit on  $\text{BR}(\mu \rightarrow e\gamma)$  and show that, in some cases, this may help to restrict the SUSY parameter space, as well as to set complementary limits on the seesaw scale.

**KEYWORDS:** Supersymmetry; Neutrino masses and mixing; Lepton flavour violation

---

## Contents

<b>1</b>	<b>Introduction</b>	<b>1</b>
<b>2</b>	<b>Models</b>	<b>3</b>
2.1	Supersymmetric seesaw type I	3
2.2	Supersymmetric seesaw type II	4
2.3	Supersymmetric seesaw type III	5
<b>3</b>	<b>Lepton flavour violation in the (s)lepton sector</b>	<b>6</b>
<b>4</b>	<b>Numerical analysis and results</b>	<b>8</b>
4.1	Setup	8
4.2	Results	10
<b>5</b>	<b>Concluding remarks</b>	<b>23</b>

---

## 1 Introduction

With the data accumulated in 2011 and 2012, both the CERN ATLAS and CMS collaborations have recently claimed the discovery of a new particle that resembles very much the long-awaited Higgs boson. The mass of this new state, measured in good accordance in different decay channels, is in the ballpark of  $m_{h^0} \simeq (123 - 127)$  GeV. While the overall significance in the 2011 data was only  $2.2\sigma$  in ATLAS [1] and  $2.1\sigma$  in CMS [2], with the 2012 update both experiments increased their statistical significances to the  $5\sigma$  discovery threshold [3, 4]. Especially noteworthy is that both ATLAS and CMS observe an excess of events in the  $\gamma\gamma$  and  $ZZ$  decay channels with an invariant mass which differs by roughly 2 GeV, i.e. consistent at the  $1\sigma$  level. Complementary evidence has been reported by the CDF and D0 experiments at the Tevatron. These collaborations have recently released updated combined results on searches for the Higgs boson [5], finding a  $\sim 3\sigma$  statistical significance in the  $b\bar{b}$  decay channel.

Given that supersymmetry (SUSY) has been the most popular paradigm for physics beyond the standard model (SM) in the last decades, the recent LHC results have triggered the expected flurry of theoretical activity dedicated to the study of how a relatively heavy Higgs constrains the supersymmetric parameter space [6–44]. The general consensus is that a lightest Higgs boson with a mass of  $m_{h^0} \sim 125$  GeV is uncomfortably heavy for *minimal* SUSY. Here, by minimal SUSY we mean a supersymmetric model with no new superfields and no new interactions, gauged or non-renormalizable, at the electroweak scale. In this framework, the hefty Higgs requires either multi-TeV scalar tops or very large stop

mixing [7, 10, 16, 31, 32]. In the latter case, the lightest stop could still be relatively light, say  $m_{\tilde{t}_1} \gtrsim 500$  GeV [45]. For a constrained minimal supersymmetric standard model (CMSSM) with universal boundary conditions at a high scale, such a spectrum requires that at least one of the three basic parameters  $M_{1/2}$ ,  $m_0$  or  $A_0$  takes a minimum value of several TeV [7, 10, 31]. In addition, it has been found that a moderately large  $\tan\beta$  may be helpful to increase the Higgs boson mass [7, 10, 31].

The naturalness problem of the MSSM with a  $\sim 125$  GeV Higgs mass has revived the discussion around non-minimal supersymmetric extensions of the standard model. In particular, the recent LHC data has been scrutinized in the context of SUSY models with new F-terms (like the NMSSM) [15, 22, 26, 35, 39], extended gauge models with additional new D-terms [46–51], heavy-SUSY scenarios like Split SUSY [52–54], “natural SUSY” [33, 55–58]) and high-scale SUSY [59, 60]) or “effective” SUSY, i.e. SUSY with new non-renormalisable operators [61–64], among others. In this work, we will follow an alternative approach and assume SUSY is realized minimally. We explore the consequences of the LHC Higgs search data on the CMSSM parameter space and the SUSY spectrum, from a viewpoint similar to that taken in MSSM-dedicated studies like, for instance, the one of Ref. [10]. However, our analysis differs from these by considering that a seesaw mechanism for neutrino mass generation is implemented in the MSSM. Our motivation lies in the fact R-parity conserving MSSM (with or without CMSSM boundary conditions) does not provide an explanation for the observed neutrinos masses and, thus, is not complete.

From the theoretical point of view, implementing the seesaw mechanism in the (supersymmetric) SM seems to be the simplest (and most motivated) solution to the neutrino mass problem. With renormalizable interactions only, there are three tree-level realizations of the seesaw mechanism [65] usually called type I [66–70], II [69–75] and III [76]. These three variations differ from each other by the nature of their seesaw messengers. Namely, in type I an effective neutrino mass operator arises from the decoupling of heavy neutrino singlets, while in type II one integrates out a heavy SU(2) scalar triplet with hypercharge two. Instead, in the type III seesaw neutrino masses are generated through the tree-level exchange of SU(2) fermionic triplets of zero hypercharge. If in type II and III one extends the MSSM by just adding the superfields required to generate neutrino masses, then one of the most appealing properties of the MSSM is lost: gauge coupling unification. This stems from the fact that both the scalar and fermionic triplets belong to incomplete SU(5) representations. Unification can be easily restored by embedding those states in full SU(5) multiplets like 15-plets in the case of type II [77] or 24-plets [78] in the case of type III. Note that, in addition to the SU(2) triplet, the 24 of SU(5) contains a singlet which also contributes to the effective neutrino mass operator and, thus, the decoupling of the 24-plet leads to an admixture of type I and type III seesaws.

The main purpose of this work is to investigate whether imposing a Higgs mass around 125 GeV allows to some extent to differentiate the CMSSM from the constrained SUSY seesaws and also whether type II and III seesaws are distinguishable among themselves. We will complement this analysis by imposing the MEG constraint on the branching ratio

of the radiative lepton flavour violating decay  $\text{Br}(\mu \rightarrow e\gamma) \leq 2.4 \times 10^{-12}$  [79].

The rest of this paper is organized as follows. We start by recalling the general features of the aforementioned SUSY seesaw models in Section 2 and present some discussion related with lepton flavour violation (LFV) in Section 3. Afterwards, we describe our numerical analysis and present its results in Sections 4.1 and 4.2, respectively. Our conclusions are drawn in Section 5.

## 2 Models

In the following we will briefly describe the three types of SUSY seesaw mechanisms considered in this work and possible embedding in a grand-unified (GUT) model based on the SU(5) gauge group. We use standard notation for the MSSM superfields, namely  $L$ ,  $Q$  and  $H_u$  ( $H_d$ ) denote the lepton, quark and hypercharge one (minus one) Higgs superfields, while the lepton and quark singlets are  $E^c$ ,  $D^c$  and  $U^c$ . The vacuum expectation values of  $H_{u,d}$  are denoted by  $v_{u,d}/\sqrt{2}$  with  $\tan\beta = v_u/v_d$  and  $v = \sqrt{v_u^2 + v_d^2} = 246$  GeV.

### 2.1 Supersymmetric seesaw type I

In the case of the supersymmetric type I seesaw, very heavy singlet superfields  $N^c$  are added to the MSSM, yielding the following superpotential below the grand-unification scale  $M_{GUT}$ :

$$W_I = W_{MSSM} + W_\nu, \quad (2.1)$$

$$W_{MSSM} = \mathbf{Y}_u U^c Q H_u - \mathbf{Y}_d D^c Q H_d - \mathbf{Y}_e E^c L H_d + \mu H_u H_d, \quad (2.2)$$

$$W_\nu = \mathbf{Y}_\nu N^c L H_u + \frac{1}{2} \mathbf{M}_R N^c N^c, \quad (2.3)$$

where SU(2)-invariant products are implicit. This model can be realized in an SU(5) framework taking the following SU(5) matter representations:  $1 = N^c$ ,  $\bar{5}_M = \{D^c, L\}$  and  $10_M = \{Q, U^c, E^c\}$ . At the effective level, a dimension five neutrino mass operator of the type  $LLH_u H_u$  originates from the decoupling of the heavy singlets, leading to an effective neutrino mass matrix given by the well-known seesaw formula

$$\mathbf{m}_\nu = -\frac{v_u^2}{2} \mathbf{Y}_\nu^T \mathbf{M}_R^{-1} \mathbf{Y}_\nu, \quad (2.4)$$

after electroweak symmetry breaking (EWSB). Being complex symmetric,  $\mathbf{m}_\nu$  is diagonalized by a  $3 \times 3$  unitary matrix  $\mathbf{U}$  [69]

$$\hat{\mathbf{m}}_\nu = \mathbf{U}^T \mathbf{m}_\nu \mathbf{U}. \quad (2.5)$$

The lepton mixing matrix  $\mathbf{U}$  can be parameterized in the standard form

$$\mathbf{U} = \begin{pmatrix} c_{12}c_{13} & s_{12}c_{13} & s_{13}e^{-i\delta} \\ -s_{12}c_{23} - c_{12}s_{23}s_{13}e^{i\delta} & c_{12}c_{23} - s_{12}s_{23}s_{13}e^{i\delta} & s_{23}c_{13} \\ s_{12}s_{23} - c_{12}c_{23}s_{13}e^{i\delta} & -c_{12}s_{23} - s_{12}c_{23}s_{13}e^{i\delta} & c_{23}c_{13} \end{pmatrix} \begin{pmatrix} e^{i\alpha_1/2} & 0 & 0 \\ 0 & e^{i\alpha_2/2} & 0 \\ 0 & 0 & 1 \end{pmatrix}, \quad (2.6)$$

with  $c_{ij} = \cos \theta_{ij}$  and  $s_{ij} = \sin \theta_{ij}$ . The angles  $\theta_{12}$ ,  $\theta_{13}$  and  $\theta_{23}$  are the solar, the reactor (or CHOOZ) and the atmospheric neutrino mixing angle, respectively, while  $\delta$  is the Dirac phase and  $\alpha_{1,2}$  are Majorana phases.

It is well known that the Dirac neutrino Yukawa couplings  $\mathbf{Y}_\nu$  can be defined in terms of the physical neutrino parameters, up to an orthogonal complex matrix  $\mathbf{R}$  [80],

$$\mathbf{Y}_\nu = \sqrt{2} \frac{i}{v_u} \sqrt{\hat{\mathbf{M}}_R \mathbf{R} \sqrt{\hat{\mathbf{m}}_\nu} \mathbf{U}^\dagger, \quad (2.7)$$

where  $\hat{\mathbf{m}}_\nu$  and  $\hat{\mathbf{M}}_R$  are diagonal matrices containing the light and heavy neutrino masses, respectively. It is worth noting that, in the special case of  $\mathbf{R} = \mathbf{1}$ , the non-trivial flavour structure of  $\mathbf{Y}_\nu$  stems from the lepton mixing matrix  $\mathbf{U}$ .

## 2.2 Supersymmetric seesaw type II

In the type II seesaw, neutrino mass generation is triggered by the tree-level exchange of scalar triplets. Its simplest SUSY version requires the addition of a vector-like pair of SU(2) triplet superfields  $T$  and  $\bar{T}$  of hypercharge  $Y = \pm 2$ . A natural way to implement the type II seesaw in a GUT scenario is to embed the triplets in a 15 and  $\bar{15}$ -plet of SU(5) which decompose under  $SU(3) \times SU(2) \times U(1)$  in the following way [77]

$$\begin{aligned} 15 &= S + T + Z, \\ S &\sim (6, 1, -2/3), \quad T \sim (1, 3, 1), \quad Z \sim (3, 2, 1/6), \end{aligned} \quad (2.8)$$

with an obvious decomposition for the  $\bar{15}$ . The SU(5) invariant superpotential reads

$$\begin{aligned} W &= \frac{1}{\sqrt{2}} \mathbf{Y}_{15} \bar{5} 15 \bar{5} + \frac{1}{\sqrt{2}} \lambda_1 \bar{5}_H 15 \bar{5}_H + \frac{1}{\sqrt{2}} \lambda_2 5_H \bar{15} 5_H + \mathbf{Y}_5 10 \bar{5} \bar{5}_H \\ &+ \mathbf{Y}_{10} 10 10 5_H + M_{15} 15 \bar{15} + M_5 \bar{5}_H 5_H, \end{aligned} \quad (2.9)$$

with  $5_H = (H^c, H_u)$  and  $\bar{5}_H = (\bar{H}^c, H_d)$ . We do not go through the details of the SU(5) breaking as we take the above SU(5) realization only as a guideline to fix some of the boundary conditions at  $M_{GUT}$ . Below  $M_{GUT}$ , in the SU(5)-broken phase, the superpotential reads

$$\begin{aligned} W_{II} &= W_{MSSM} + \frac{1}{\sqrt{2}} (\mathbf{Y}_T L T L + \mathbf{Y}_S D^c S D^c) + \mathbf{Y}_Z D^c Z L \\ &+ \frac{1}{\sqrt{2}} (\lambda_1 H_d T H_d + \lambda_2 H_u \bar{T} H_u) + M_T T \bar{T} + M_Z Z \bar{Z} + M_S S \bar{S}. \end{aligned} \quad (2.10)$$

The dimension five effective neutrino mass originates now from the decoupling of the triplet states, leading to an effective neutrino mass matrix

$$\mathbf{m}_\nu = \frac{v_u^2}{2} \frac{\lambda_2}{M_T} \mathbf{Y}_T, \quad (2.11)$$

once electroweak symmetry is spontaneously broken. It is apparent from the above equation that the flavour structure of  $\mathbf{m}_\nu$  at low energies is the same as the one of the couplings  $\mathbf{Y}_T$

at the decoupling scale  $M_T$  (up to renormalization group effects which can be relevant in some special cases [81]). Consequently,  $\mathbf{Y}_T$  is diagonalized by the same matrix as  $\mathbf{m}_\nu$ , i.e.

$$\hat{\mathbf{Y}}_T = \mathbf{U}^T \mathbf{Y}_T \mathbf{U}. \quad (2.12)$$

In short, if all neutrino eigenvalues, angles and phases were known,  $\mathbf{Y}_T$  would be fixed up to an overall constant which can be easily estimated to be

$$\frac{M_T}{\lambda_2} \simeq 10^{15} \text{GeV} \left( \frac{0.05 \text{ eV}}{m_\nu} \right). \quad (2.13)$$

In principle, the remaining *flavoured* Yukawa couplings  $\mathbf{Y}_S$  and  $\mathbf{Y}_Z$  are not determined by any low-energy neutrino data. Still, they both induce LFV slepton mass terms, just as  $\mathbf{Y}_T$  does. Having the above SU(5) GUT model in mind, we impose the unification condition  $\mathbf{Y}_T = \mathbf{Y}_S = \mathbf{Y}_Z$  at  $M_{GUT}$  in our numerical analysis presented in Section 4. As for the heavy-state masses, the mass equality condition  $M_T = M_Z = M_Z = M_{15}$  imposed at the GUT scale is spoiled by the renormalization group (RG) running of the masses. Nevertheless, these effects are small and, therefore, gauge coupling unification is maintained. In view of this, for practical purposes we decouple the  $T$ ,  $Z$  and  $S$  states at the common scale  $M_T(M_T)$ , neglecting in this way threshold effects resulting from the small RG-induced splittings among the heavy masses.

### 2.3 Supersymmetric seesaw type III

In the case of a type III seesaw model, neutrino masses are generated by the tree-level exchange of zero hypercharge fermions, usually denoted as  $\Sigma$ , belonging to the adjoint representation of SU(2). These states can be accommodated, for instance, in a 24-plet of SU(5) [82]. Above the SU(5) breaking scale, the relevant superpotential for our discussion is

$$W = \sqrt{2} \mathbf{Y}_5 \bar{5}_M 10_M \bar{5}_H - \frac{1}{4} \mathbf{Y}_{10} 10_M 10_M 5_H + \mathbf{Y}_{24} 5_H 24_M \bar{5}_M + \frac{1}{2} \mathbf{M}_{24} 24_M 24_M. \quad (2.14)$$

As in the type II case, we do not specify the Higgs sector responsible for the SU(5) breaking. The superpotential terms directly involved in neutrino mass generation are those containing the representations  $24_M$ , which decompose under  $\text{SU}(3) \times \text{SU}(2) \times \text{U}(1)$  as

$$\begin{aligned} 24_M &= (1, 1, 0) + (8, 1, 0) + (1, 3, 0) + (3, 2, -5/6) + (3^*, 2, 5/6), \\ &= N^c + G + \Sigma + X + \bar{X}. \end{aligned} \quad (2.15)$$

The fermionic components of  $(1, 1, 0)$  and  $(1, 3, 0)$  have the same quantum numbers as  $N^c$  (the type I heavy neutrino singlets) and  $\Sigma$ . Thus, one expects that, in general, the decoupling of the  $24_M$  components leads to an effective neutrino mass operator which contains both a type I and a type III seesaw contribution. In the SU(5) broken phase the superpotential is

$$\begin{aligned} W_{III} &= W_{MSSM} + H_u \left( \mathbf{Y}_\Sigma \Sigma - \sqrt{\frac{3}{10}} \mathbf{Y}_\nu N^c \right) L + \mathbf{Y}_X H_u \bar{X} D^c \\ &\quad + \frac{1}{2} \mathbf{M}_R N^c N^c + \frac{1}{2} \mathbf{M}_G G G + \frac{1}{2} \mathbf{M}_\Sigma \Sigma \Sigma + \mathbf{M}_X X \bar{X}. \end{aligned} \quad (2.16)$$

Once more, we impose the GUT scale boundary condition  $\mathbf{Y}_\Sigma = \mathbf{Y}_\nu = \mathbf{Y}_X$  and  $\mathbf{M}_R = \mathbf{M}_G = \mathbf{M}_\Sigma = \mathbf{M}_X$ . Integrating out the heavy fields, and after EWSB, the following effective neutrino mass matrix is generated:

$$\mathbf{m}_\nu = -\frac{v_u^2}{2} \left( \frac{3}{10} \mathbf{Y}_\nu^T \mathbf{M}_R^{-1} \mathbf{Y}_\nu + \frac{1}{2} \mathbf{Y}_\Sigma^T \mathbf{M}_\Sigma^{-1} \mathbf{Y}_\Sigma \right). \quad (2.17)$$

As mentioned above, there are two contributions to neutrino masses stemming from the gauge singlets  $N^c$  as well as from the SU(2) triplets  $\Sigma$ . In this case the extraction of the Yukawa couplings from low-energy parameters for a given high scale spectrum is more complicated than in the other two types of seesaw models. However, as we start from universal couplings and masses at  $M_{GUT}$ , we find that at the seesaw scale one still has  $\mathbf{M}_R \simeq \mathbf{M}_\Sigma$  and  $\mathbf{Y}_\nu \simeq \mathbf{Y}_\Sigma$ . Consequently, one has

$$\mathbf{m}_\nu \simeq -v_u^2 \frac{4}{10} \mathbf{Y}_\Sigma^T \mathbf{M}_\Sigma^{-1} \mathbf{Y}_\Sigma, \quad (2.18)$$

to a good approximation. This result allows us to use the same decomposition for  $\mathbf{Y}_\Sigma$  as the one discussed in section 2.1, up to the overall factor 4/5 [see Eq. (2.7)].

### 3 Lepton flavour violation in the (s)lepton sector

The search for LFV processes beyond neutrino oscillations has attracted a great deal of attention both from the experimental and theoretical communities. Rare decays like  $\mu \rightarrow e\gamma$  have been searched for decades, without any positive result. The most stringent constraint on this process comes from the MEG experiment [83] which, by analysing the data collected in 2009 and 2010 [79], has set the new bound  $\text{Br}(\mu \rightarrow e\gamma) < 2.4 \cdot 10^{-12}$ .

The branching ratio (BR) for  $l_i \rightarrow l_j\gamma$  can be generically written as [84]

$$\text{Br}(l_i \rightarrow l_j\gamma) = \frac{48\pi^3\alpha}{G_F^2} \left( |\mathbf{A}_L^{ij}|^2 + |\mathbf{A}_R^{ij}|^2 \right) \text{Br}(l_i \rightarrow l_j\nu_i\bar{\nu}_j). \quad (3.1)$$

The amplitudes  $\mathbf{A}_L$  and  $\mathbf{A}_R$  depend on the specific physics framework and, in general, are generated at the 1-loop level. In our SUSY scenario, the dependence of those amplitudes on the LFV slepton soft masses is approximately given by

$$\mathbf{A}_L^{ij} \sim \frac{(\mathbf{m}_L^2)_{ij}}{m_{SUSY}^4}, \quad \mathbf{A}_R^{ij} \sim \frac{(\mathbf{m}_{\tilde{e}^c}^2)_{ij}}{m_{SUSY}^4}, \quad (3.2)$$

where  $\mathbf{m}_L^2$  and  $\mathbf{m}_{\tilde{e}^c}^2$  are the doublet and singlet slepton soft mass matrices, respectively, and  $m_{SUSY}$  is a typical supersymmetric mass. In the derivation of these estimates one typically assumes that (a) chargino/neutralino masses are similar to slepton masses and (b) left-right flavour mixing induced by  $A$ -terms is negligible<sup>1</sup>.

---

<sup>1</sup>This assumption is not valid when large values of  $|A_0|$  are considered. Nevertheless, the above estimates can be still used to illustrate the dependence of the BRs on the low-energy neutrino parameters.

Assuming universal boundary conditions for the soft SUSY-breaking terms at the GUT scale, and considering only the leading-log approximation for the LFV slepton masses and trilinear terms induced through RG running, one obtains:

$$(\mathbf{m}_L^2)_{ij} \simeq -\frac{a_k}{8\pi^2} (3m_0^2 + A_0^2) \left( \mathbf{Y}_k^\dagger \mathbf{L} \mathbf{Y}_k \right)_{ij}, \quad (3.3)$$

$$(\mathbf{A}_e)_{ij} \simeq -a_k \frac{3}{16\pi^2} A_0 \left( \mathbf{Y}_e \mathbf{Y}_k^\dagger \mathbf{L} \mathbf{Y}_k \right)_{ij}, \quad (3.4)$$

for  $i \neq j$ . In the basis where  $\mathbf{Y}_e$  is diagonal,  $\mathbf{L}_{mn} = \ln(M_{GUT}/M_n)\delta_{mn}$  and  $\mathbf{Y}_k$  is the Yukawa coupling of the type- $k$  seesaw ( $k = I, II, III$ ) with  $\mathbf{Y}_k = (\mathbf{Y}_\nu, \mathbf{Y}_T, \mathbf{Y}_\Sigma)$ , given at  $M_{GUT}$ . Taking into account the renormalisation group equations (RGEs) for  $\mathbf{m}_L^2$  and  $\mathbf{A}_e$  we obtain

$$a_I = 1, \quad a_{II} = 6 \text{ and } a_{III} = 9/5. \quad (3.5)$$

Note, that in case of the type II seesaw the matrix  $\mathbf{L}$  is proportional to the identity and thus can be factored out. All models considered here have in common that they predict negligible flavour violation for the RH sleptons

$$(\mathbf{m}_{\tilde{e}^c}^2)_{ij} \simeq 0. \quad (3.6)$$

Although not very accurate, the above approximations allow to estimate the LFV slepton masses and  $A$ -terms within different seesaw frameworks. The BRs for rare lepton decays  $l_i \rightarrow l_j \gamma$  are roughly given by

$$\text{Br}(l_i \rightarrow l_j \gamma) \propto \alpha^3 m_{l_i}^5 \frac{|(\mathbf{m}_L^2)_{ij}|^2}{m_{SUSY}^8} \tan^2 \beta. \quad (3.7)$$

For distinct seesaw scenarios, and a given set of high-scale parameters, the above BRs change due to the different  $(\mathbf{m}_L^2)_{ij}^2$  and the distorted mass spectrum (which differs from the pure CMSSM one). The most important parameter turns out to be the seesaw scale due to its influence on the size of the Yukawas. The higher the seesaw scale is, the larger are the Yukawa couplings and, consequently, the LFV rates. In case of the type II seesaw, the coupling  $\lambda_2$  plays a crucial rôle, as seen in Eq. (2.13). Small values of this parameter lead to large  $\mathbf{Y}_T$  Yukawa couplings and high LFV rates.

Finally, we would like to comment on the influence of the  $\mathbf{R}$  matrix on LFV decay rates. As shown in Eq. (2.7), the  $\mathbf{Y}_\nu$  Yukawa couplings for type I seesaw are proportional to  $\mathbf{R}$  and, thus, different choices of this matrix lead to different off-diagonal entries in the soft squared mass terms (which in turn changes the LFV rates). Similarly, the type III Yukawa couplings,  $\mathbf{Y}_\Sigma$ , follow an analogous equation and, consequently, also change with  $\mathbf{R}$ . This additional freedom can be used to cancel some  $\left( \mathbf{Y}_k^\dagger \mathbf{L} \mathbf{Y}_k \right)_{ij}$  combinations, in particular the one with  $(i, j) = (\mu, e)$  [80]. This allows for large LFV effects in the  $\tau - e$  and  $\tau - \mu$  sectors while having negligible  $\mu - e$  transitions. In the following, we will disregard this



possibility<sup>2</sup>. Therefore, implications on  $M_{SS}$  drawn from  $\mu \rightarrow e\gamma$  considerations can be regarded as approximate lower bounds<sup>3</sup>.

## 4 Numerical analysis and results

### 4.1 Setup

Our numerical results have been obtained with **SPheno** [87, 88]. Taking as input the SM parameters, as well as the usual universal soft terms at the GUT scale

$$m_0, M_{1/2}, A_0, \tan \beta, \text{sign}(\mu), \quad (4.1)$$

**SPheno** computes the resulting SUSY spectrum by means of complete 2-loop RGEs [89–91], properly adapted for every model. This includes the pure CMSSM and the three seesaw variants studied in this work. At the SUSY scale, the  $\mu$  parameter is obtained including the most relevant 2-loop corrections [92] and complete 1-loop corrections to all sparticle masses are implemented [93]. These calculations follow the  $\overline{DR}$  renormalization scheme.

In case of the Higgs boson mass, the aforementioned 1-loop corrections are supplemented by the most relevant  $\mathcal{O}[\alpha_s(\alpha_t + \alpha_b) + (\alpha_t + \alpha_b)^2 + \alpha_\tau\alpha_b + \alpha_\tau^2]$  2-loop contributions [92, 94–98]. For a detailed study of the **SPheno** results for the Higgs boson mass and a comparison to other popular numerical codes we refer to [98]. We have checked that our results agree, within the usual 2 – 3 GeV theoretical uncertainty, with the results given by **FeynHiggs** [99]. This code uses an on-shell renormalization scheme and therefore small differences are expected on theoretical grounds. In particular, larger differences are found for very large Higgs boson masses,  $m_{h^0} \sim 129 - 130$  GeV, a region where numerical computations are no longer accurate.

Uncertainties in the Higgs mass calculation have been often discussed in the literature. In short, the dominant sources of the theoretical error on  $m_{h^0}$  are the uncertainty in the top (bottom) mass, the missing (sub-dominant) 2-loop contributions and the missing dominant 3-loop diagrams in public codes. Currently, the Particle Data Group quotes  $m_t = 173.5 \pm 1.0$  [100], leading to  $\Delta m_{h^0} \lesssim 1$  GeV, depending on the parameter point. We note in passing that a complete 2-loop calculation based on the Higgs effective potential exists in the literature [101]. Moreover, 3-loop contributions to the Higgs mass have also been calculated [102, 103]. So far, none of these contributions [101–103] have been implemented into a public code.

---

<sup>2</sup>In fact, we will always consider real parameters and degenerate spectra for the right-handed (RH) neutrinos (in type I) and for the SU(2) fermion triplets (in type III). In such scenarios the  $\mathbf{R}$  matrix is physically irrelevant, since it drops out in the computation of  $\left(\mathbf{Y}_k^\dagger \mathbf{L} \mathbf{Y}_k\right)_{ij}$  [80]. For a discussion on the effects of considering complex parameters we address the reader to, e.g. Refs. [85, 86].

<sup>3</sup>Once  $\text{Br}(\mu \rightarrow e\gamma)$  and  $m_{\tilde{\nu}} \sim m_{SUSY}$  are known, one can determine  $M_{SS}$  assuming  $\mathbf{R} = \mathbf{1}$ . Under this assumption, an upper limit on  $\text{Br}(\mu \rightarrow e\gamma)$  can lead to an upper limit on  $M_{SS}$ , once  $m_{\tilde{\nu}} \sim m_{SUSY}$  is (at least approximately) known. Larger  $M_{SS}$  are in principle possible if  $\mathbf{R}$  is tuned to obtain a cancellation in the  $\mu - e$  sector. However, one cannot find  $\mathbf{R}$  matrices that allow to go to much smaller  $M_{SS}$  scales.

We also found good agreement between our results and those presented in some recent works devoted to the study of the Higgs mass in the MSSM [7, 10, 31, 43]. Although the theoretical error is always present, and the exact numbers might differ in some cases, the general behaviour and the dependence on the SUSY parameters are correctly reproduced. We have decided not to compute the SUSY spectrum at a fixed scale  $Q = 1$  TeV, as suggested by the SPA conventions [104], since that is known to give a poor accuracy in the determination of the Higgs boson mass for scenarios with very large values of  $A_0$  or with multi-TeV stop masses. Instead, we compute the SUSY spectrum at the geometric average of the two stop masses  $m_{\tilde{t}_{1,2}}$ , i.e.  $M_S = \sqrt{m_{\tilde{t}_1} m_{\tilde{t}_2}}$ .

Although we evaluate the Higgs mass numerically taking into account the higher-order corrections enumerated above, we find it useful to recall that the leading 1-loop corrections to the Higgs mass for moderate values of  $\tan\beta$  and large Higgs pseudoscalar mass  $m_A$ , are approximately given by [105–108]

$$m_{h^0} \simeq m_Z^2 \cos^2 \beta + \frac{3m_t^4}{4\pi^2 v^2} \left[ \ln \left( \frac{M_S^2}{m_t^2} \right) + \frac{X_t^2}{M_S^2} \left( 1 - \frac{X_t^2}{12M_S^2} \right) \right], \quad X_t = A_t - \mu \cot \beta, \quad (4.2)$$

where  $\mu$  is the Higgsino mass parameters,  $A_t$  is the top trilinear term at low-energy and  $X_t$  is the mixing parameter in the stop sector. Obviously, the above approximation is not always very accurate. In any case, we will only use it to understand the behaviour of the Higgs mass with some of the input parameters of the seesaw models discussed in the previous section.

In the following we will present and discuss our numerical results. Notice that we will loosely talk about “the seesaw scale”,  $M_{SS}$ , when referring to the mass of the seesaw mediators, i.e. the right-handed neutrino mass,  $M_R$ , in case of seesaw type I, the  $Y = 2$  triplet mass,  $M_{15}$  (or  $M_T$ ), for type II or the mass of the  $Y = 0$  triplet,  $M_{24}$  (or  $M_\Sigma$ ), for type III. Our assumptions regarding the input parameters for each of the seesaw models are:

**Type I:** We consider the general case of 3 degenerate RH neutrinos with mass  $M_R$ . In the flavour sector, we fix  $\mathbf{R} = \mathbf{1}$  [see Eq. (2.7)]. This choice does not have a significant impact on the Higgs mass since, as already pointed out, the effect of the Yukawa couplings on  $m_{h^0}$  is marginal. As shown below, even the model with three copies of degenerate RH neutrinos is always very close to the CMSSM limit. Therefore, we will not discuss variants with less RH neutrinos or with non-degenerate masses.

**Type II:** Apart from the unification conditions for the Yukawa couplings and masses of the different 15-plet components mentioned in Section 2.2, we will use in most of the cases the values  $\lambda_{1,2}(M_{GUT}) = 0.5$  for the superpotential couplings of the triplets with the Higgs superfields. Later, we will comment on how relaxing this condition affects the Higgs and squark masses.

**Type III:** We will always assume the existence of three copies of 24-plets, with an approximately degenerate mass  $M_\Sigma$ . Alternatively, one could also explain neutrino data

with two degenerate 24's or with three, being one “light” and the other two close to the GUT scale. The first of these options leads to results somewhere between those shown for type II and type III with three degenerate 24's, while the latter has  $m_{h^0}$  somewhere between type II and type I. Since nothing qualitatively new results from these cases, we will not discuss them in detail. As in the type I case we assume  $\mathbf{R} = \mathbf{1}$ .

For all our numerical cases the values of the low-energy neutrino parameters (mixing angles and mass-squared differences) coincide with the best-fit values provided by global analysis of all neutrino oscillation data [109–111]. To simplify our analysis, we consider all couplings and mass parameters to be real and for  $\tan\beta$  we take the reference value  $\tan\beta = 20$ . For other values of  $\tan\beta$ , our CMSSM results agree quite well with those discussed, for example, in [10]. We have scanned the parameters  $m_0$  and  $M_{1/2}$  in the range of  $[0, 10]$  TeV. As for  $A_0$ , we have taken values in the interval  $[-5, 5]$  TeV, although we will mainly concentrate on the two extreme cases with  $A_0 = 0$  TeV and  $A_0 = -5$  TeV. For other choices of  $A_0$  (and  $\tan\beta$ ) the results always lie between the extreme ones, as discussed in detail for the CMSSM in Refs. [10, 43]. Since our findings agree with these works, we do not repeat the discussion here.

Current bounds on squark and gluino masses in CMSSM-like setups from ATLAS [112] and CMS [113] already exclude  $m_{\tilde{g}} = m_{\tilde{q}} \simeq 1.4$  TeV and  $m_{\tilde{g}} \simeq (800 - 900)$  GeV for very heavy squarks. Therefore, we will mainly concentrate on parts of the parameter space where  $m_{\tilde{g}}$  and  $m_{\tilde{q}}$  are larger than 1 TeV.

There are several other constraints on SUSY from different searches in the literature. However, as shown below, our spectra are always relatively heavy and, therefore, they pass all other known experimental constraints (once we impose the Higgs mass window). Of particular importance is the recent upper limit on  $B_s^0 \rightarrow \mu^+\mu^-$  [114], which particularly constrains the large  $\tan\beta$  region of the SUSY parameter space [115]. Since in our numerical examples we use the moderate value  $\tan\beta = 20$ , the  $B_s^0 \rightarrow \mu^+\mu^-$  bound is not exceeded.

## 4.2 Results

It is well known that adding seesaw mediators with masses between the SUSY and GUT scales changes the RG running of gauge couplings. As a result, the RG flow of all Yukawa couplings and mass parameters is modified with respect to the CMSSM case [116–120]. In the case of type II and III seesaws, the increase in the value of the common gauge coupling  $\alpha(M_{GUT})$  leads, in general, to lighter sparticles [116, 117]. Therefore, one expects the Higgs mass to be sensitive to the parameters characterising each seesaw model, namely the mass  $M_{SS}$  and possible couplings with the Higgs and/or lepton sectors of the MSSM. Consequently, the reconstruction of the SUSY-breaking parameters at the universality scale  $M_{GUT}$  from low-energy mass measurements will be very sensitive to the presence of new fields at intermediate scales.

As an example, in Fig. 1 we show the behaviour of the stop masses  $m_{\tilde{t}_{1,2}}$  and mixing parameter  $X_t$ , as well as the mass of the lightest Higgs,  $h^0$ , as a function of the seesaw scale  $M_{SS}$ , for seesaw type I (blue), type II (red) and type III (black) taking  $m_0 = 0.5$  TeV and

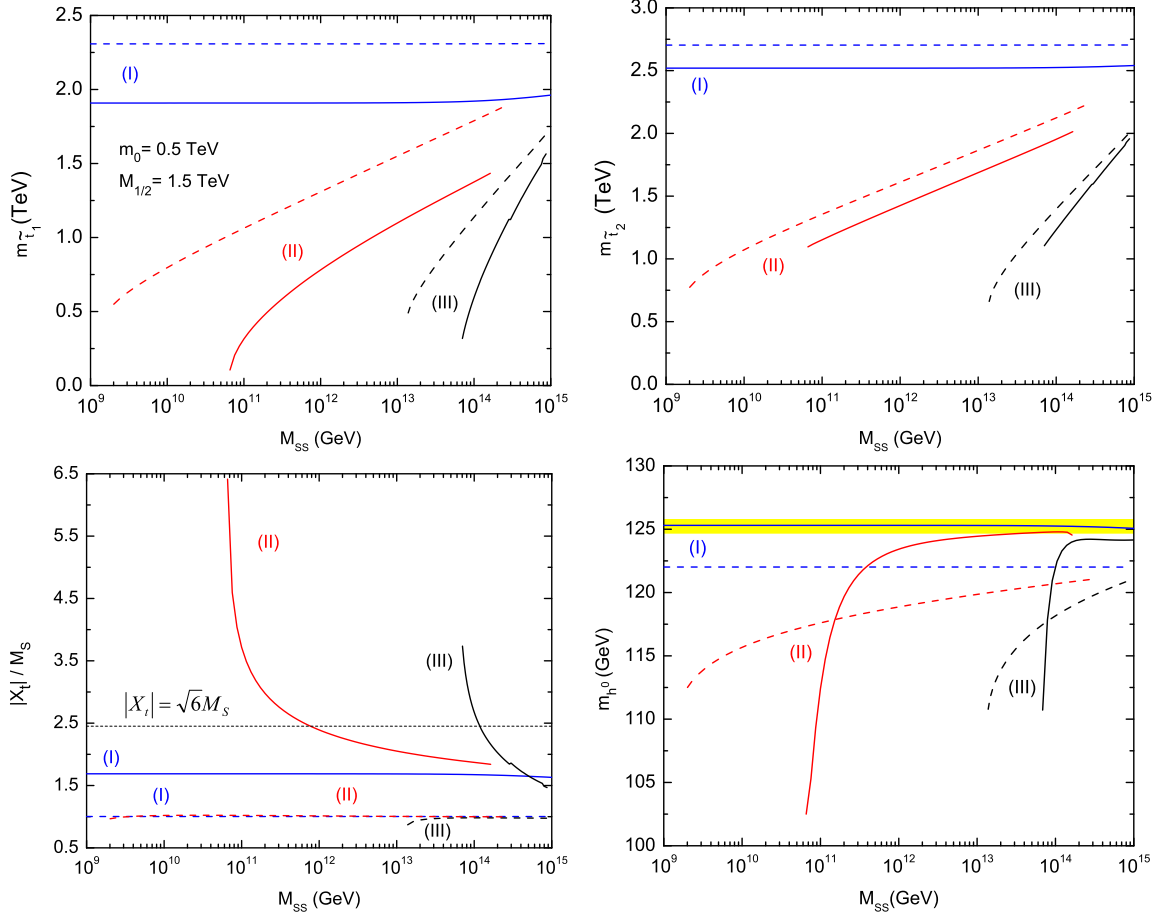


**Figure 1.** Variation of the scalar top masses (top panels), the ratio  $|X_t/M_S|$  and the mass of the lightest Higgs  $h^0$  (bottom panels) with  $M_{SS}$ , for a particular point in the SUSY parameter space with  $m_0 = 0.5$  TeV,  $M_{1/2} = 1.5$  TeV. The blue, red and black lines correspond to seesaw type I, II and III, respectively. The results are shown for  $A_0 = 0$  TeV (dashed lines) and  $A_0 = -3$  TeV (solid lines). For values of the seesaw scale larger than roughly  $10^{15}$  GeV no solutions consistent with observed neutrino data can be found. Also, for  $M_{SS} \lesssim (\text{few}) 10^9$  [ $10^{13}$ ] GeV gauge couplings become non-perturbative below the GUT scale in case of seesaw type II [type III]. See also text.

$M_{1/2} = 1.5$  TeV. The results are shown for two values of the common trilinear term at the GUT scale, namely  $A_0 = -3$  TeV (solid lines) and  $A_0 = 0$  TeV (dashed lines). For values of the seesaw scale larger than roughly  $10^{15}$  GeV no solutions consistent with observed neutrino data can be found, while for values of the seesaw scale below approximately (few)  $10^9$  ( $10^{13}$ ) GeV gauge couplings become non-perturbative below the GUT scale in case of seesaw type II (type III). This explains why no results are shown for lower values of  $M_{SS}$  in those cases.

The first immediate (and expected) conclusion that one can infer from the results presented in this figure is that there is essentially no dependence of  $m_{h^0}$  on  $M_R$  in case of type I (bottom-right panel in Fig. 1). This is due to the fact that sparticle masses do not

change with  $M_R$ , as can be seen for the particular cases of  $m_{\tilde{t}_{1,2}}$  (top panels) and neither stop mixing does. Due to the singlet nature of the RH neutrinos in the type I seesaw, and to the fact that they only have Yukawa couplings  $\mathbf{Y}_\nu$  with the lepton and Higgs doublet superfields [see Eq. (2.1)] the soft SUSY breaking MSSM parameters affected at the 1-loop level are  $m_{H_u}^2$ ,  $\mathbf{m}_L^2$ ,  $\mathbf{A}_e$  and  $\mathbf{A}_u$ . Still, even those show only very mild departures from their CMSSM values. All other soft masses change only at the 2-loop level.

The neutrino Yukawas  $\mathbf{Y}_\nu$  required to fit neutrino data depend on  $M_R$  and are  $\mathcal{O}(1)$  for  $M_R \simeq 10^{15}$  GeV. The results of all plots in Fig. 1 show that, even for such large Yukawas, the changes of the SUSY spectrum are relatively small, due to the *short* RG running from the GUT scale to  $M_R$ .<sup>4</sup> For smaller values of  $M_R$  no traces of the seesaw remain in the SUSY spectrum [122]. The only important consequence of changing  $M_R$  is the strong effect of this scale on the LFV entries of  $\mathbf{m}_L^2$  which control the rates of LFV processes like  $\mu \rightarrow e\gamma$  (see Section 3 and the discussion below). Moreover, as the results of Fig. 1 show, changing the value of  $A_0$  from zero to -3 TeV, shifts down the stop masses (middle left panel) due to the term proportional to  $A_t^2$  in the RGE of  $(\mathbf{m}_{\tilde{u}c}^2)_{33}$ . On the other hand, the magnitude of the stop mixing parameter  $X_t$  increases as a consequence of the fact that, at low energies,  $|A_t|$  is larger for  $A_0 = -3$  TeV than for  $A_0 = 0$  TeV. Therefore,  $|X_t/M_S|$  increases when going from vanishing  $A_0$  to  $A_0 = -3$  TeV, resulting in an increase of the Higgs mass by approximately 3 GeV. Of course, this feature is also present in the CMSSM and is by no means related with the presence of the heavy neutrino singlets.

The situation changes when one turns to the type II and type III seesaws. In these cases, for a fixed choice of CMSSM parameters, one usually finds that stop masses become smaller when lowering the seesaw scale,  $M_{SS}$ . At the same time, the stop mixing angle can increase. However, this increase is practically never sufficient to compensate for the smaller stop masses. Thus, in general,  $m_{h^0}$  decreases with decreasing  $M_{SS}$  for both type II and type III. As Fig. 1 shows this decrease depends also on  $A_0$ , with changes in  $m_{h^0}$  being much smoother (and smaller) for  $A_0 = 0$  TeV than for  $A_0 = -3$  TeV. For the lowest values of  $M_{SS}$  possible,  $m_{h^0}$  can be even lighter for  $A_0 = -3$  TeV than for  $A_0 = 0$  TeV. This is due to the rather strong dependence of the stop masses on  $A_0$ . All these features, discussed here for a special CMSSM point, are qualitatively valid for rather larger ranges on the CMSSM parameter space, as we will discuss next.

In Fig. 2 we show examples of squark mass, Higgs mass and  $\text{Br}(\mu \rightarrow e\gamma)$  contours in the plane  $(m_0, M_{1/2})$  for CMSSM plus seesaw type I, taking two extreme values of the seesaw scale  $M_R$ , namely  $10^9$  GeV (top) and  $10^{14}$  GeV (bottom); as well as two values of  $A_0$ :  $A_0 = 0$  TeV (left) and  $A_0 = -5$  TeV (right). Here, and in the corresponding figures for type-II and type-III seesaw (Figs. 3 and 5, respectively), we show contours of  $m_{h^0}$  in the range 124 – 128 GeV, which corresponds very roughly to the theoretical allowed range for

<sup>4</sup>A shift of  $m_{h^0}$  of the order of several GeV was found in [121] in case of type-I seesaw, if the soft SUSY breaking mass term  $m_M$  for the right-sneutrinos is of the order of  $M_R$ . For  $m_M \sim m_{SUSY} \sim \mathcal{O}(\text{few TeV})$  (as it is in our case), the shift in the Higgs mass is always less than  $\mathcal{O}(0.1)$  GeV, i.e. far below the theoretical uncertainty of the calculation.

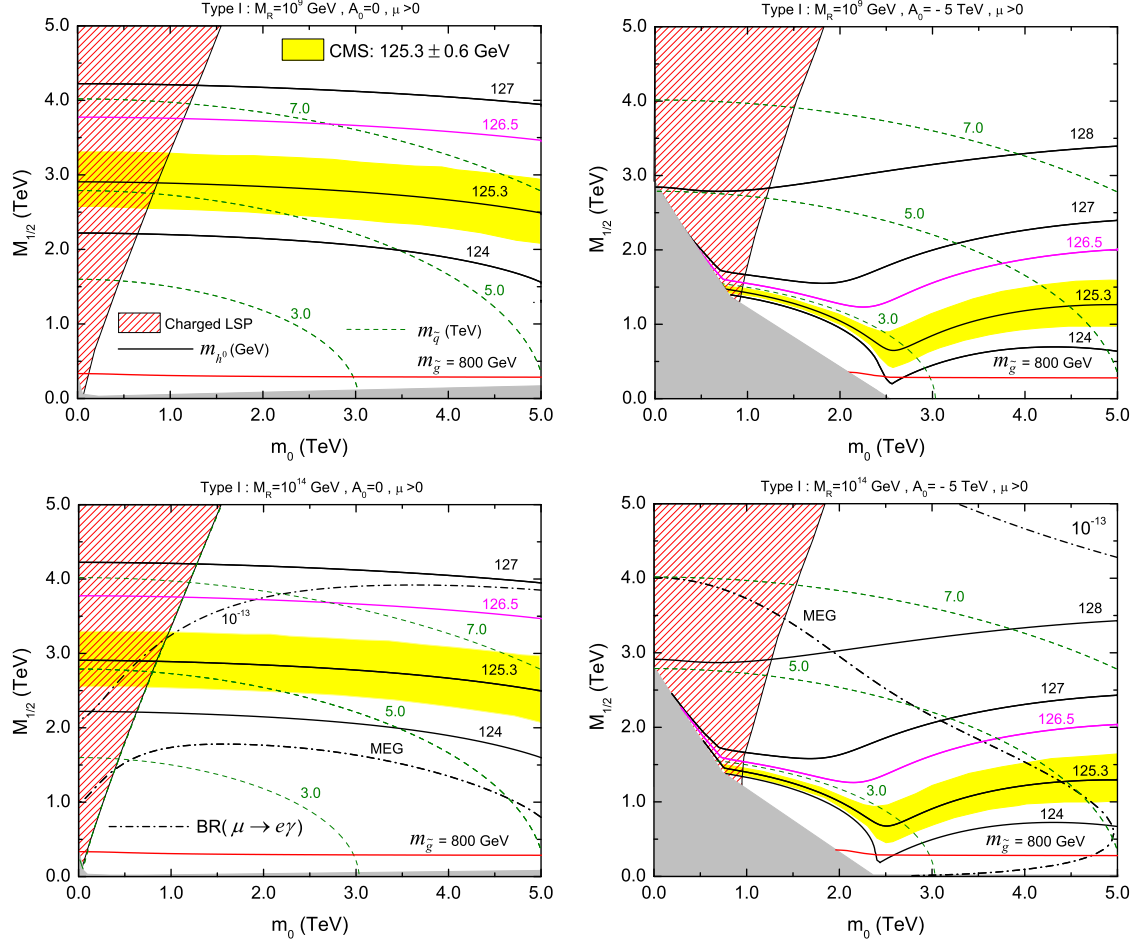


**Figure 2.** Examples of squark mass, Higgs mass and  $\text{Br}(\mu \rightarrow e\gamma)$  contours in the plane  $(m_0, M_{1/2})$  for CMSSM plus seesaw type I for two values of the seesaw scale  $M_R$ :  $M_R = 10^9$  GeV (top) and  $M_R = 10^{14}$  GeV (bottom); as well as two values of  $A_0$ :  $A_0 = 0$  TeV (left) and  $A_0 = -5$  TeV (right).  $\text{Br}(\mu \rightarrow e\gamma)$  is orders of magnitude below the expected experimental sensitivity in case of  $M_R = 10^9$  GeV and, therefore, contours are not shown (for a discussion see text).

a calculated  $m_{h^0} = 126$  GeV. The hatched regions on the left lead to a charged LSP and, thus, are not acceptable due to cosmological constraints (charged dark matter). In the grey regions, EWSB is not possible in a consistent way. The solid lines show contours of  $m_{h^0}$  at 124, 125.3 (central CMS value), 126.5 (central ATLAS value) and 127 GeV, to reflect the currently favoured region of  $m_{h^0}$ . The green dashed lines correspond to constant average squark masses, defined as

$$m_{\tilde{q}} = \frac{m_{\tilde{d}_L} + m_{\tilde{d}_R}}{2}, \quad (4.3)$$

while the (black) dash-dotted lines refer to the contours  $\text{Br}(\mu \rightarrow e\gamma) = 2.4 \times 10^{-12}$  (MEG) and  $10^{-13}$ . The yellow region corresponds to values of  $m_{h^0}$  in the CMS interval  $125.3 \pm 0.6$  GeV. Below the red solid line  $m_{\tilde{g}} < 800$  GeV.

For  $m_{h^0} = 125$  GeV we find squark masses in the range of typically 5 TeV for  $A_0 =$



0 TeV and as low as 2 TeV for  $A_0 = -5$  TeV. However, considerably larger squark masses,  $\mathcal{O}(10)$  TeV, can be found in the CMS preferred window of Higgs mass. This is consistent with the findings of previous works on the CMSSM [7, 10, 31] and in agreement with expectations. If this scenario is indeed realized in nature one expects to observe squarks at the LHC with  $\sqrt{s} = 14$  TeV (LHC14) only for the largest values of  $A_0$ . Still, even for  $A_0 = -5$  TeV large parts of the allowed parameter space in squark and gluino masses will remain unexplored by LHC14.

Fig. 2 shows also contours of  $\text{Br}(\mu \rightarrow e\gamma)$  assuming (a) a degenerate RH neutrino spectrum with  $\mathbf{R} = \mathbf{1}$  (see Section 2.1) and (b) low-energy neutrinos fitted with a normal hierarchy spectrum and mixing angles within the allowed range [109]. It is well-known that different choices of  $\theta_{13}$  can lead to values of  $\text{Br}(\mu \rightarrow e\gamma)$  differing by a considerable factor [123, 124]. However, we fix  $\theta_{13}$  according to the results of [109], where a global fit to all available experimental data gives a best-fit value of  $\sin^2 \theta_{13} = 0.026$  in case of a neutrino spectrum with normal hierarchy. We note that with degenerate RH neutrinos and  $\mathbf{R} = \mathbf{1}$ , a complete cancellation of  $\text{Br}(\mu \rightarrow e\gamma)$  is no longer possible within the  $3\sigma$  allowed range of  $\sin^2 \theta_{13}$  [109]. In case of  $M_R = 10^9$  GeV,  $\text{Br}(\mu \rightarrow e\gamma)$  is orders of magnitude below the expected experimental sensitivity and, thus, contours are not shown. However, if  $M_R = 10^{14}$  GeV,  $\text{Br}(\mu \rightarrow e\gamma)$  is well within the current expected sensitivity of MEG. Therefore, for the CMSSM with a seesaw type I and  $m_{h^0} = 125$ , MEG already provides an upper limit on  $M_R$  of the order of  $10^{14}$  GeV, despite the fact that sleptons in the CMSSM are relatively heavy in the allowed parameter space. We notice that the constraints from  $\text{Br}(\mu \rightarrow e\gamma)$  are, in general, more stringent for large values of  $A_0$ .

In Fig. 3 we show the results in the plane  $(m_0, M_{1/2})$  for type II seesaw with  $M_T = 10^9, 10^{14}$  GeV and  $A_0 = 0, -5$  TeV. When  $M_T = 10^{14}$  GeV, the results for  $m_{h^0}$  and the squark masses are very similar to the CMSSM ones, although some small shifts are visible upon closer inspection (see also below). On the other hand, the contours for  $\text{Br}(\mu \rightarrow e\gamma)$  are different from those in Fig. 2. This is in agreement with expectations [116, 125], since in type I neutrino masses scale as the square of the Yukawa couplings whereas in type II neutrino masses are linearly proportional to  $\mathbf{Y}_T$  [see Eqs. (2.4) and (2.11)], while the RG running of the LFV soft masses depends quadratically on the Yukawas in both cases. Note, that in Fig. 3 we have used  $\lambda_2 = 0.5$ . A value of  $\lambda_2 = 1$  would lead to smaller values of  $\text{Br}(\mu \rightarrow e\gamma)$  by (roughly) a factor of four. Much larger values of  $\lambda_2$  are not allowed, if the theory is to remain perturbative up to the GUT scale.

For  $M_T = 10^9$  GeV, on the other hand, the results look drastically different. All Higgs (and squark) mass contours are shifted to larger values of  $m_0$  and  $M_{1/2}$ . This is in agreement with the previous observation that lower values of the seesaw scale lead to lighter particles for the same point in CMSSM parameter space (see discussion of Fig. 1). As a consequence, the Higgs becomes lighter. To compensate for this downward shift in the SUSY spectrum one has to increase the parameters  $m_0$  and/or  $M_{1/2}$ . However, while a low type II scale now requires very large  $m_0$  and/or  $M_{1/2}$ , the resulting squark (and gluino) contours in the interesting range of  $m_{h^0}$  are similar to those found in the CMSSM. This

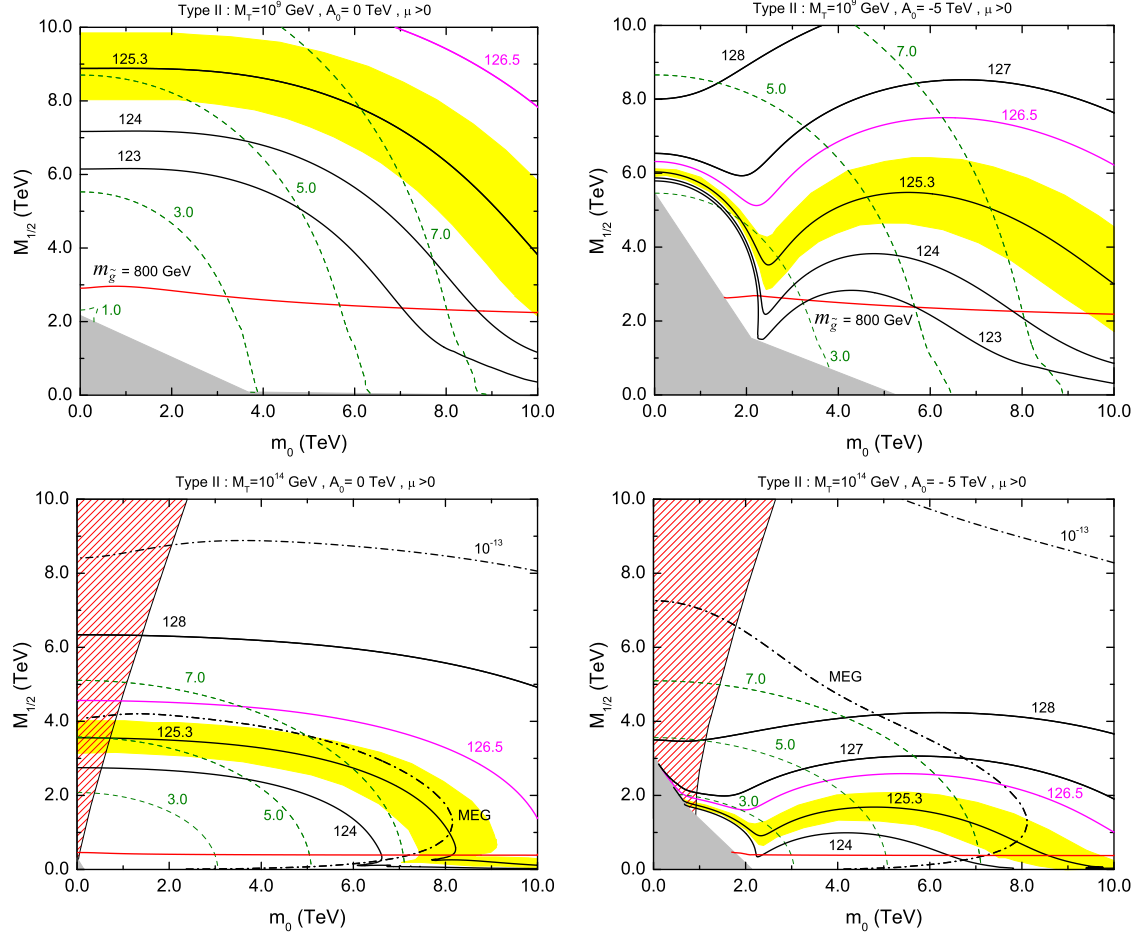


**Figure 3.** Squark mass, Higgs mass and  $\text{Br}(\mu \rightarrow e\gamma)$  contours in the plane  $(m_0, M_{1/2})$  for CMSSM plus seesaw type II for two values of the seesaw scale  $M_T$ :  $M_T = 10^9$  GeV (top) and  $M_T = 10^{14}$  GeV (bottom); as well as two values of  $A_0$ :  $A_0 = 0$  TeV (left) and  $A_0 = -5$  TeV (right). The values of  $\text{Br}(\mu \rightarrow e\gamma)$  are orders of magnitude below the expected experimental sensitivity in case of  $M_T = 10^9$  GeV and, thus, are not shown. Note the change in scale compared to Fig. 2 (for further discussion see text).

stems from the fact that  $m_{h^0} = 125$  GeV requires again squark masses in the range of (at least) 5 TeV for  $A_0 = 0$  TeV and 2 TeV for  $A_0 = -5$  TeV. This is not surprising since the Higgs mass is sensitive only to physical masses and mixings. However, as we will discuss below, there are some potentially interesting differences in the spectra due to the different RG running in the CMSSM and the SUSY type II seesaw.

For the lowest value of  $M_T$ , where the spectrum distortions are larger,  $\text{Br}(\mu \rightarrow e\gamma)$  is again negligible. Thus, an upper limit on  $\text{Br}(\mu \rightarrow e\gamma)$  provides an upper limit on  $M_T$  for any given value of the Higgs mass. A measurement of  $\text{Br}(\mu \rightarrow e\gamma)$  fixes a combination of  $\lambda_2$  and  $M_T$  for fixed  $m_{h^0}$ . On the other hand, a lower limit on  $m_{h^0}$  provides a lower limit on a combination of  $m_0$ ,  $M_{1/2}$  and  $A_0$  for any fixed choice of  $M_T$ . Note that, contrarily to what happens in type I and III, in type II seesaw (with a single 15-plet pair) low-energy



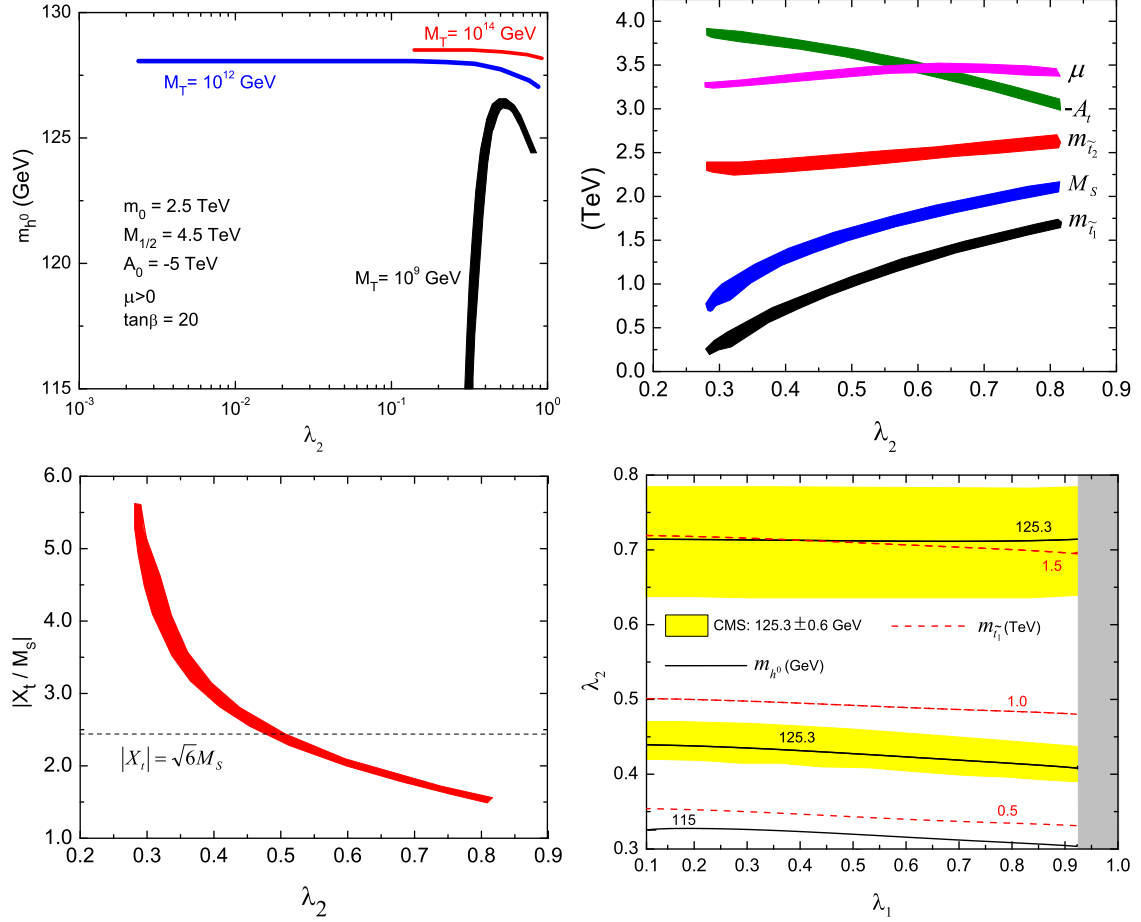


**Figure 4.** Dependence of several low-energy SUSY parameters on the couplings  $\lambda_{1,2}$  for the type II seesaw scenario. The results are shown for a specific point in the SUSY parameter space with  $m_0 = 2.5$  TeV,  $M_{1/2} = 4.5$  TeV,  $A_0 = -5$  TeV,  $\tan\beta = 20$  and  $\mu > 0$ . Top left: Higgs mass as a function of  $\lambda_2$  for  $M_T = 10^9$  GeV (black),  $M_T = 10^{12}$  GeV (blue) and  $M_T = 10^{14}$  GeV (red). Top right:  $\lambda_2$  dependence of the stop masses  $m_{\tilde{t}_{1,2}}$  (and their geometric average  $M_S$ ), the Higgsino mass parameter  $\mu$  and the top-trilinear term  $A_t$ . Bottom left: stop mixing parameter  $X_t$  as function of  $\lambda_2$ . Bottom right: contours of the Higgs (black solid) and lightest stop (red dashed) masses in the  $(\lambda_1, \lambda_2)$  plane for  $M_T = 10^9$  GeV. The yellow regions corresponds to the CMS Higgs mass interval  $m_{h^0} = 125.3 \pm 0.6$  GeV. There are two CMS allowed contours in the lower right plot, since  $m_{h^0}$  first increases then decreases with  $\lambda_2$  for  $M_T = 10^9$  GeV, compare to the figure in the upper left.

neutrino parameters essentially determine  $\mathbf{Y}_T$  in a way that large cancellations in the LFV soft masses are not possible. Moreover, when LFV in the soft masses is generated by  $\mathbf{Y}_T$  only, the large value of  $\sin\theta_{13}$  provided by the latest global analysis of neutrino oscillation data together with the present MEG bound on  $\mu \rightarrow e\gamma$  set an upper limit on the radiative  $\tau$  decays  $\tau \rightarrow \mu(e)\gamma$  which is out of the reach of future experiments [77, 81, 116, 126–128].

In the SUSY type II seesaw, the heavy triplet states  $T$  and  $\bar{T}$  couple to the MSSM Higgs sector through the superpotential couplings  $\lambda_{1,2}$  [see Eq. (2.10)]. We therefore expect these parameters to affect the Higgs mass to some extent. Obviously, since  $T$  and  $\bar{T}$  are

very heavy, the effect of  $\lambda_{1,2}$  on the low-energy SUSY masses is indirect and originates from RG corrections induced on the SUSY parameters between  $M_{GUT}$  and  $M_T$ . Consequently, these corrections are typically larger for smaller  $M_T$ . In Fig. 4 we show the dependence of several parameters relevant for the computation of  $m_{h^0}$  as a function of  $\lambda_1$  and  $\lambda_2$  (taken at the scale  $M_T$ ), for a specific point of the SUSY parameter space (see caption). In the top-left panel we show a plot of  $m_{h^0}$  versus  $\lambda_2$  (and varying  $\lambda_1$  from 0.1 to the maximum allowed by perturbativity) for  $M_T = 10^9, 10^{12}, 10^{14}$  GeV. As expected, the impact of  $\lambda_2$  on the Higgs mass is only significant for the case with  $M_T = 10^9$  GeV. In the remaining two examples, a mild dependence on  $\lambda_2$  is observed when the value of this parameter is very close to the Landau pole. From this plot one can also conclude that the effect of  $\lambda_1$  on  $m_{h^0}$  is small, since the thickness of the lines (which reflects the variation of  $m_{h^0}$  on  $\lambda_1$ ) is not too pronounced. In view of this, we will only comment on the  $\lambda_2$ -dependence of  $m_{h^0}$  for  $M_T = 10^9$  GeV.

The top-right panel of Fig. 4 shows the variation of some relevant parameters with  $\lambda_2$  (see caption for more details). We first note that while  $\mu$  and  $m_{\tilde{t}_{1,2}}$  (and consequently  $M_S$ ) increase with increasing  $\lambda_2$ ,  $|A_t|$  decreases (here  $A_t$  is always negative since  $A_0 < 0$ ). This behaviour can be qualitatively understood by looking at the type II seesaw RGEs for the soft masses and trilinear terms. In particular, we notice that the RGE for  $A_t$  contains a term proportional to  $|\lambda_2|^2 A_t$  which, at leading-log approximation, induces a correction to the top trilinear given by

$$\Delta A_t = -\frac{3y_t|\lambda_2|^2}{8\pi^2} A_0 \ln\left(\frac{M_{GUT}}{M_T}\right), \quad (4.4)$$

which is positive for  $A_0 < 0$ . This explains why  $-A_t$  decreases with  $\lambda_2$  and, consequently, why  $X_t$  decreases<sup>5</sup>. The behaviour of  $\mu$  can be traced taking into account that the Higgs soft masses  $m_{H_{d,u}}^2$  receive a contribution which amounts to:

$$\Delta m_{H_{d,u}}^2 = -\frac{9m_0^2 + 3A_0^2}{8\pi^2} |\lambda_{1,2}|^2 \left(\frac{M_{GUT}}{M_T}\right). \quad (4.5)$$

Notice that, if not too small, the parameter  $\lambda_1$  can act on  $m_{H_d}^2$  as the top Yukawa coupling does on  $m_{H_u}^2$  bringing it to negative values at low-energies. In fact, we observe that for  $\lambda_1$  large,  $m_{H_d}^2$  is also negative at the EW scale. We recall from the EWSB symmetry breaking condition:

$$\mu^2 = \frac{m_{H_d}^2 - \tan^2 \beta m_{H_u}^2}{\tan^2 \beta - 1} - \frac{m_Z^2}{2}. \quad (4.6)$$

As  $\lambda_2$  increases,  $m_{H_u}^2$  becomes more negative and  $m_{H_d}^2$  decreases, going from positive to negative values. This leads to an increasing of the value of  $\mu$  with  $\lambda_2$ .

Although not affected directly by  $\lambda_2$ , the stop masses  $m_{\tilde{t}_{1,2}}$  (and, thus, the dynamical scale  $M_S$ ) increases with that parameter mainly due to positive RG corrections in  $(\mathbf{m}_{\tilde{Q},\tilde{u}^c})_{33}$ . The results for  $|X_t/M_S|$  as function of  $\lambda_2$  are shown in the bottom-left panel of Fig. 4.

---

<sup>5</sup>Notice that in this case  $X_t \sim -A_t$  since  $\mu \sim -A_t$  and  $\cot \beta = 0.05$ .

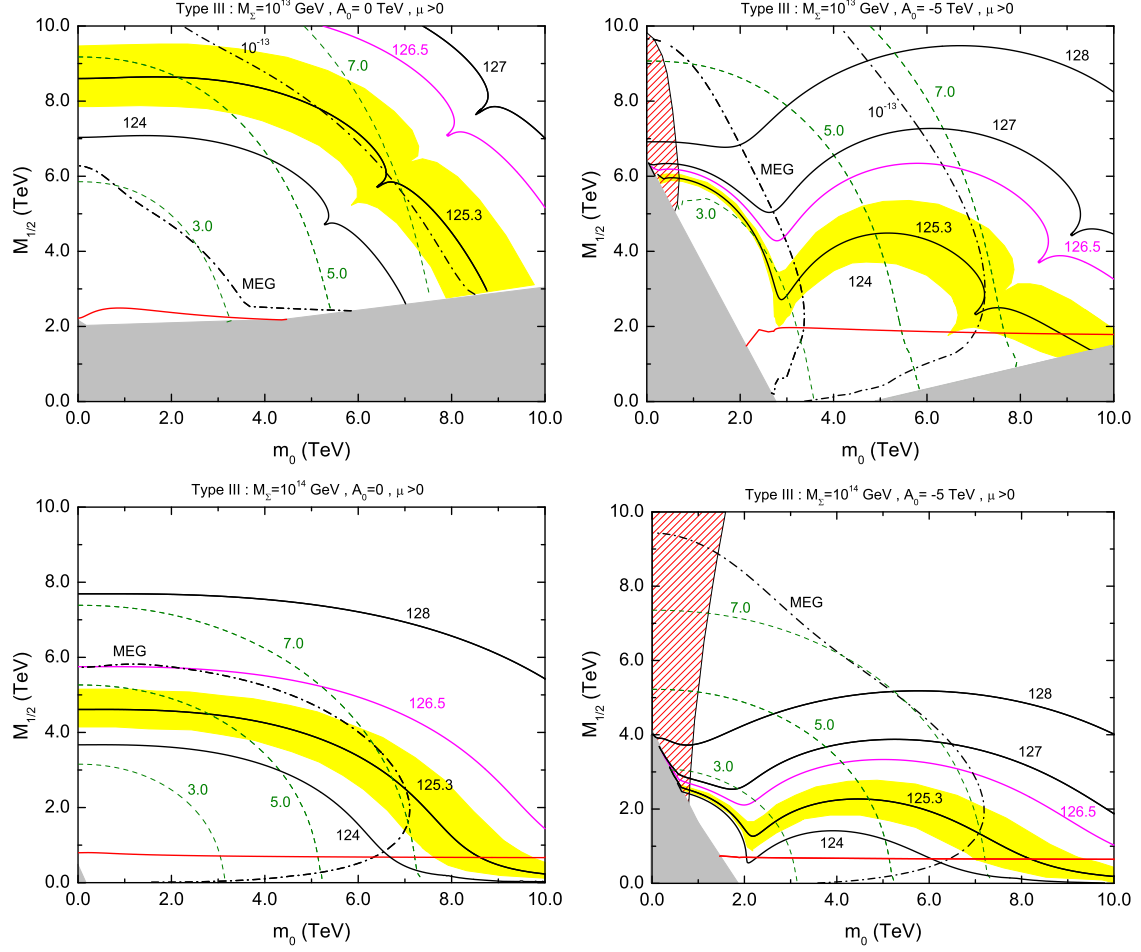


**Figure 5.** Examples of squark mass, Higgs mass and  $\text{Br}(\mu \rightarrow e\gamma)$  contours in the plane  $(m_0, M_{1/2})$  for CMSSM plus seesaw type III for two values of the seesaw scale  $M_{SS}$ :  $M_\Sigma = 10^{13}$  GeV (top) and  $M_{SS} = 10^{14}$  GeV (bottom); as well as two values of  $A_0$ :  $A_0 = 0$  TeV (left) and  $A_0 = -5$  TeV (right). For a discussion see text.

Together with Eq. (4.2), these results allow us to understand the behaviour of  $m_{h^0}$  with  $\lambda_2$  shown in the top-left panel. In particular, we stress that for  $\lambda_2 \simeq 0.5$  we have  $|X_t| = \sqrt{6}M_S$ , which corresponds to the “maximal mixing” scenario with maximised  $m_{h^0}$  (see the top-left panel). Finally, in the bottom-right panel, the contours of  $m_{h^0}$  and  $m_{\tilde{t}_1}$  are shown in the  $\lambda_{1,2}$  plane for  $M_T = 10^9$  GeV. The results confirm that while both  $m_{h^0}$  and  $m_{\tilde{t}_1}$  depend reasonably strong on  $\lambda_2$ , their dependence on  $\lambda_1$  is almost negligible. In particular, the effect of  $\lambda_2$  on  $m_{h^0}$  can be much larger than its theoretical uncertainty.

In Fig. 5 we show the results in the  $(m_0, M_{1/2})$  plane for type III seesaw with  $M_\Sigma = 10^{13}, 10^{14}$  GeV. For lower values of the 24-plet mass no solutions consistent with perturbativity exist. Since in type III all SUSY masses run strongly towards smaller values when  $M_\Sigma$  is lowered, already for  $M_\Sigma = 10^{13}$  GeV the spectrum distortions with respect to the type I case are as large (or larger) as those found for type II with  $M_T = 10^9$  GeV (compare

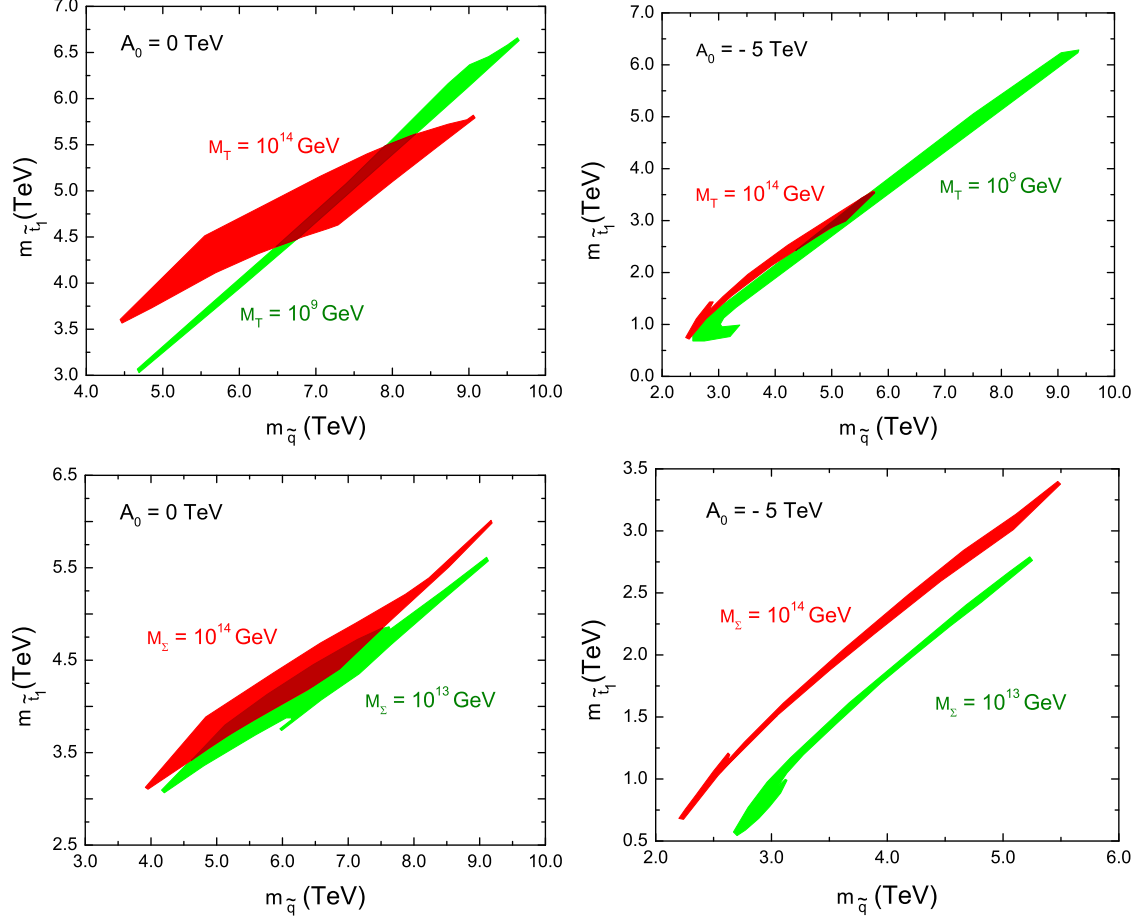


**Figure 6.** Allowed ranges of the lightest stop versus squark mass compatible with a  $125.3 \pm 0.6$  GeV Higgs (CMS range) for type II (top) and type III (bottom) seesaws with  $A_0 = 0$  TeV (left) and  $A_0 = -5$  TeV (right). The red (green) regions are for  $M_{T,\Sigma} = 10^{14}$  ( $M_T = 10^9$  GeV and  $M_\Sigma = 10^{13}$ ) GeV.

Figs. 3 and 5). As in type I and II, multi-TeV squarks (and gluinos) are required to explain  $m_{h^0} \simeq 125$  GeV. Still, depending on  $M_\Sigma$ , the relations among sparticle masses are changed. It is interesting to note that  $\text{Br}(\mu \rightarrow e\gamma)$  provides a particularly strong constraint for type III [117, 129]. In case of  $M_\Sigma = 10^{14}$  GeV (bottom plots in Fig. 5), an improvement of  $\text{Br}(\mu \rightarrow e\gamma)$  to the level of  $\simeq 10^{-13}$  (within the reach of MEG) would exclude the type III seesaw with degenerate 24-plets,  $\mathbf{R} = \mathbf{1}$  and a Higgs mass lying in the ATLAS and CMS range. In the particular case of  $A_0 = -5$  TeV (bottom-right plot) most of the CMS preferred region (in yellow) is already excluded by the constraint from MEG, which also excludes squark masses below  $\sim 7$  TeV.

We now turn to a discussion on differences found in the physical masses for the different seesaw setups. Since for type I the spectra are practically the same as in the CMSSM (which has been discussed at length in the literature) we focus on type II and III seesaws in the following. In Fig. 6 we show the allowed ranges for the lightest stop mass  $m_{\tilde{t}_1}$  and the

	$m_0$ [TeV]	$M_{1/2}$ [TeV]	$A_0$ [TeV]	$\tan \beta$	$\text{sign}(\mu)$	$M_{SS}$ [GeV]
Point I	3	3	0	20	+	$10^{14}$
Point II	7	7	0	20	+	$10^9$

**Table 1.** Benchmark points with heavy squarks and gluino. Point I corresponds to a type I seesaw and point II to a type II seesaw. Both points have been chosen to give a Higgs mass of approximately  $m_{h^0} = 125$  GeV.

average squark mass, defined in Eq. (4.3), for seesaws of type II and III with a Higgs mass in the CMS range  $125.3 \pm 0.6$  GeV (the same range is considered in Fig. 7)<sup>6</sup>. The allowed regions for the masses correspond to an uncertainty of only 0.6 GeV in the Higgs mass calculation. In view of the different outputs provided by different numerical codes (see the discussion at the beginning of Section 4.1), this is certainly too optimistic at present. The allowed ranges of masses shown in Figs. 6 and 7 should therefore be considered only as rough estimates. The red regions are for  $M_{T,\Sigma} = 10^{14}$  GeV and the green ones for  $M_T = 10^9$  GeV and  $M_\Sigma = 10^{13}$  GeV. The left (right) plots are for  $A_0 = 0$  TeV ( $A_0 = -5$  TeV). Due to the CMSSM assumptions, stop and squark masses are tightly correlated, once the Higgs mass is fixed. It is interesting to note that once  $A_0$  is also set, the requirement that the Higgs mass falls into the CMS window leads to mass combinations which show a clear dependence on the seesaw scale. Especially noteworthy is the fact that no overlap between the regions with  $M_\Sigma = 10^{14}$  GeV and  $M_\Sigma = 10^{13}$  GeV exists in case of  $A_0 = -5$  TeV. Similar allowed mass ranges are obtained for seesaw type II. However, in this case we observe some overlap between the combinations of masses, even for the extreme cases of seesaw scales shown. It is nevertheless interesting that type III with a scale as low as  $10^{13}$  GeV does not allow squark and stop masses as large as type II does. For large values of  $A_0$  and fixed  $m_{h^0}$ , part of the parameter space is testable at the LHC with  $\sqrt{s} = 14$  TeV. However, the allowed combinations of squark and stop mass for  $A_0 = 0$  TeV are completely out of range of LHC14.

Since in all our different setups large squark (and gluino) masses are required in order to explain a 125 GeV Higgs, the expectations are that no direct signals for SUSY will be found in the near future. The LHC reach for  $\sqrt{s} = 14$  TeV and 300 (3000) fb<sup>-1</sup> has been recalculated very recently in [131]. The main conclusions of this study are that, via gluino/squark searches, LHC14 will be able to explore SUSY masses up to  $m_{\tilde{g}} \sim 3.2$  TeV (3.6 TeV) for  $m_{\tilde{q}} \sim m_{\tilde{g}}$  and of  $m_{\tilde{g}} \sim 1.8$  TeV (2.3 TeV) for  $m_{\tilde{q}} \gg m_{\tilde{g}}$  with 300 fb<sup>-1</sup> (3000 fb<sup>-1</sup>). Thus, for  $m_{h^0} \sim 125$  GeV, only a small part of the allowed parameter space will be probed. However, future plans for the LHC envisage the possibility of ramping up the center-of-mass energy to  $\sqrt{s} = 33$  TeV [132]. With such a huge gain in energy, considerably larger regions of the parameter space allowed in our examples would become testable.

<sup>6</sup>While this paper was in the review process, the ATLAS collaboration released the result  $m_{h^0} = 126.0 \pm 0.4 \pm 0.4$  GeV [130]. Using this Higgs mass range would lead to allowed regions similar to those shown in Figs. 6 and 7, although shifted to larger masses.

Particle	Point I	Point II
$\tilde{\chi}_1^0$	1.35	0.54
$\tilde{d}_L, \tilde{s}_L, \tilde{u}_L, \tilde{c}_L$	6.2	7.3
$\tilde{d}_R, \tilde{s}_R, \tilde{u}_R, \tilde{c}_R$	6.0	7.3
$\tilde{b}_1$	5.6	6.1
$\tilde{b}_2$	5.9	7.1
$\tilde{t}_1$	4.7	5.0
$\tilde{t}_2$	5.6	6.1
$\tilde{g}$	6.2	2.7

**Table 2.** Some SUSY masses for the benchmark points given in Table 1. All masses are given in TeV. For point I (point II) we find  $m_{h^0} \simeq 125.6$  (125.1) GeV.

Production cross-section	Point I	Point II
$\tilde{t}_1 \tilde{t}_1^*$	3.47	2.08
$\tilde{q} \tilde{q}^*$	8.36	0.60
$\tilde{q} \tilde{q}$	72.6	9.59
$\tilde{q} \tilde{g}$	41.0	793
$\tilde{g} \tilde{g}$	3.49	17000

**Table 3.** Most relevant production cross-sections for the benchmark points given in Table 1. All cross-sections are given in attobarns. These numbers have been computed with `Prospino` [133].

To check this more quantitatively, we have calculated the cross sections for SUSY production at  $\sqrt{s} = 33$  TeV for some representative points using the code `Prospino` [133]<sup>7</sup>. The input parameters for two benchmark points lying inside the CMS Higgs mass range are given in Table 1. We have chosen one point for type I seesaw (point I) and one for type II seesaw (point II), although for the SUSY production cross sections only squark and gluino masses are really important, of course. The corresponding SUSY spectra and some production cross sections are given in Tables 2 and 3, respectively. Point I has been deliberately chosen to give  $m_{\tilde{q}} \simeq m_{\tilde{g}} \simeq 6$  TeV, while point II leads to a heavier squark spectrum (around 7 TeV) but a lighter gluino. From Table 3 one can see that point I (point II) would yield around  $\sim 40$  ( $\sim 5300$ ) squark/gluino events for an integrated luminosity of  $300 \text{ fb}^{-1}$ . These numbers are without any cuts and, therefore, should be taken as rough estimates. Nevertheless, they serve to illustrate how LHC33 would be able to cover most of the region of interest. This is also confirmed by Fig. 7 where we show the allowed regions in the  $(m_{\tilde{q}}, m_{\tilde{g}})$  plane with  $m_{h^0}$  in the CMS interval, and two extreme values of  $M_{SS}$ , for type II seesaw (top) and type III seesaw (bottom). In the left (right) panel  $A_0 = 0$  TeV ( $A_0 = -5$  TeV).

As before, we conclude that different seesaw models lead to distinct allowed combina-

<sup>7</sup>The calculation of SUSY cross section at such large c.m.s. energy requires extrapolation of the measured PDFs and, therefore, is probably only a rough estimate.

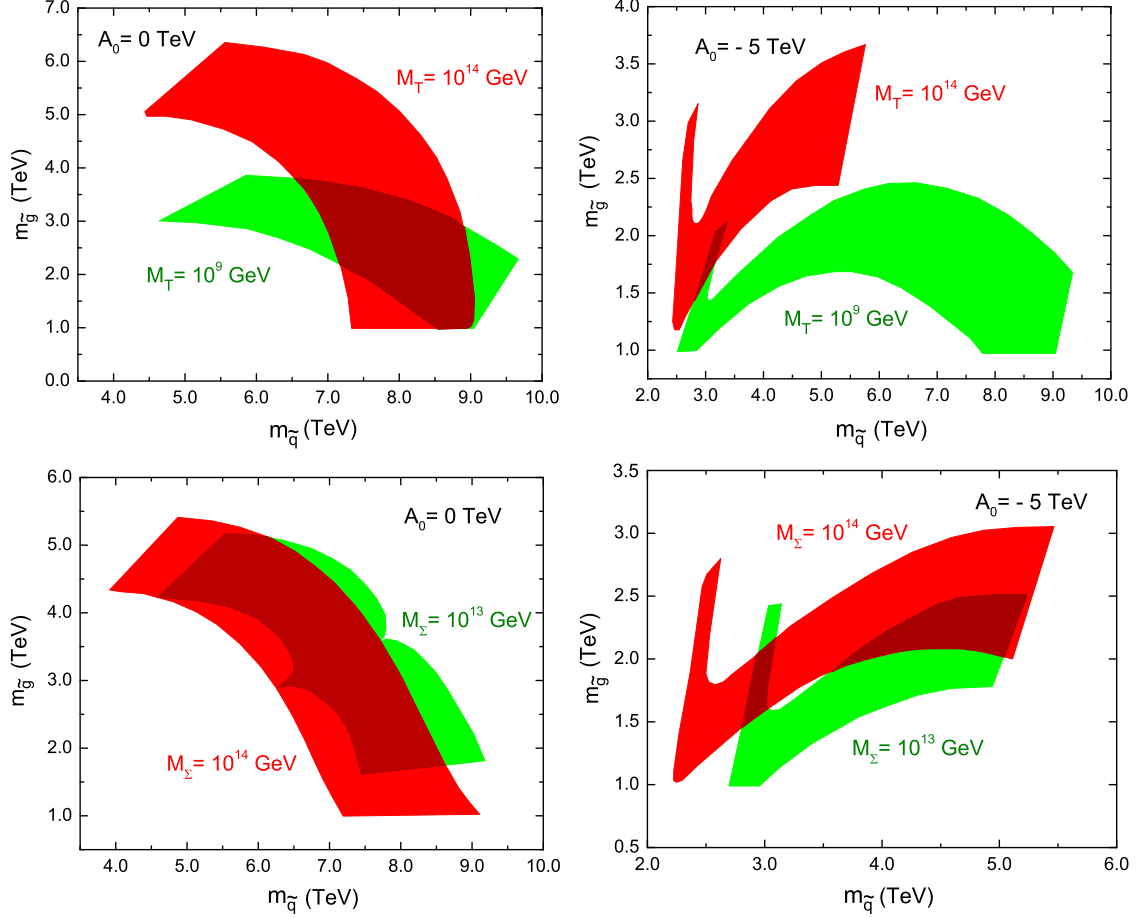


**Figure 7.** Allowed regions in the  $(m_{\tilde{q}}, m_{\tilde{g}})$  plane for seesaw type II (top) and III (bottom). In the left (right) panels  $A_0 = 0$  TeV ( $A_0 = -5$  TeV). We consider two extreme values of the seesaw scale in all cases as well as a fixed interval for the Higgs mass, namely  $m_{h^0} = 125.3 \pm 0.6$  GeV. For a discussion see text.

tions of masses. Still, in these plots, large overlaps between the regions for fixed  $A_0$  and different  $M_{SS}$  are observed. Nevertheless, we find it especially encouraging that in type II and III seesaws gluino masses should be within the reach of LHC33 in almost all cases, for a Higgs mass in the CMS preferred window. The results also show that when  $M_T = 10^9$  GeV ( $M_T = 10^{14}$  GeV),  $m_{\tilde{g}} \lesssim 4.0$  TeV ( $m_{\tilde{g}} \lesssim 6.4$  TeV) for  $A_0 = 0$  TeV. Instead, smaller values for the gluino mass are found if  $A_0 < 0$ . The corresponding numbers for type III seesaw are  $m_{\tilde{g}} \leq 5.1$  TeV ( $m_{\tilde{g}} \leq 5.4$  TeV) for  $M_\Sigma = 10^{13}$  GeV ( $M_\Sigma = 10^{14}$  GeV) and  $A_0 = 0$  TeV. These values should be compared with those of type I seesaw/pure-CMSSM where gluino masses can be as large as  $m_{\tilde{g}} \lesssim 7$  TeV for  $A_0 = 0$  TeV.

A word of caution should be added to this discussion, owing to the fact that the upper limit on  $m_{\tilde{g}}$  shown in Fig. 7 is very sensitive to the choice of the range for  $m_{h^0}$ . In particular, if the Higgs mass is as large as  $m_{h^0} = 128$  GeV, which is currently not excluded, gluino masses up to 10 TeV and larger, would be allowed. Also, for small values of  $\tan \beta$ , say in



the window  $\tan\beta \simeq (1-7)$ , loop corrections to the Higgs mass are known to be small. This would again require much heavier stops and, therefore, much heavier gluinos to explain a  $m_{h^0} \simeq 125$  GeV.

## 5 Concluding remarks

In this work we have computed the mass of the lightest Higgs boson within the three tree-level realizations of SUSY seesaws and studied the main features of these models in light of the recent ATLAS and CMS results on Higgs mass searches. We have also complemented our analysis by considering the MEG bound on the LFV radiative decay  $\mu \rightarrow e\gamma$ . As in the pure CMSSM case, in SUSY seesaws a Higgs mass in the range  $(125-126)$  GeV (as preferred currently by CMS and ATLAS [3, 4]) requires in all cases a rather heavy SUSY spectrum. This is expected since  $m_{h^0}$  is only sensitive to low-energy masses and mixings, and not to high-energy seesaw parameters (at least in a direct way). In other words, one can in principle find a different set of input parameters for each seesaw model leading to the same value of the Higgs mass. For this reason, a possible seesaw discrimination cannot rely on the Higgs mass data alone. Still, one expects to observe some differences in the physical low-energy SUSY spectrum.

We have discussed squark, stop and gluino masses preferred by the current Higgs data in the different seesaw scenarios. While some small part of the parameter space allowed by a hefty Higgs will be tested at LHC14, most of our points are beyond the reach of the next LHC run. However, a possible increase of the LHC energy to  $\sqrt{s} = 33$  TeV [132] would make it possible to cover a large part of the parameter space allowed by the current Higgs data in our models. By considering some benchmark scenarios, we have also concluded that, in some cases, the allowed regions in the squark/stop and squark/gluino planes do not overlap when different values of the seesaw scale are considered or distinct seesaws are compared. Although this is not a general feature of the models under study, we believe this kind of analysis may be useful in the future to distinguish among seesaw setups and/or set limits on the input parameters of a particular model. Complementary information coming from the flavour sector, namely from rare decay searches, can also play a crucial rôle in the accomplishment of this task. In particular, upcoming data from MEG (and also from other LFV dedicated experiments) will certainly lead to further restrictions on the seesaw parameter space.

We would like to mention that current data [3, 4] prefers an enhanced branching ratio for the di-photon final state;  $\sigma^{\text{obs}}/\sigma^{\text{SM}} = 1.54 \pm 0.43$  for CMS  $1.9 \pm 0.5$  for ATLAS. With our heavy SUSY spectrum such an enhancement can not be explained. However, currently this “discrepancy” is only of the order of  $(1-2)\sigma$  and thus not significant.

In this work we have not considered dark matter constraints (for a study of neutralino dark matter in the type-II and type-III seesaw setups considered in this paper, we address the reader to Refs. [117, 134]). Although dark matter is known to provide powerful constraints on the SUSY parameter space, one should keep in mind that these constraints are



only valid if a standard thermal history for the early universe is assumed (see for example [135]). There have also been several works devoted to the study of whether lepton flavour violation can be probed at the LHC (some examples within SUSY seesaw are [136–138]). We have not taken this possibility into account, simply because in our framework the Higgs mass constraint leads to SUSY spectra which are too heavy to allow measuring LFV at the LHC with any reasonable statistics.

Finally, we would like to remark that, although at low-energies the CMSSM may not seem very different from its seesaw variants, the reconstruction of the initial conditions do drastically change from one case to the other. In view of this, one should reflect about the meaningfulness of fitting the CMSSM input parameters in a context where neutrino masses cannot be explained, as it happens to be in the MSSM. Low-energy measurements do result on different preferred regions for the input parameters when distinct models are considered. Obviously, this is not relevant for phenomenological studies at low energies, but it is surely crucial for studies addressing the dynamics behind SUSY breaking.

## Acknowledgments

We thank Werner Porod and Florian Staub for helpful discussions and assistance with SPheno. M.H. acknowledges support from the Spanish MICINN grants FPA2011-22975, MULTIDARK CSD2009-00064 and by the Generalitat Valenciana grant Prometeo/2009/091 and the EU Network grant UNILHC PITN-GA-2009-237920. F.R.J. thanks the CERN Theory Division for hospitality during the final stage of this work and acknowledges support from the EU Network grant UNILHC PITN-GA-2009-237920 and from the *Fundação para a Ciência e a Tecnologia* (FCT, Portugal) under the projects CERN/FP/123580/2011, PTDC/FIS/098188/2008 and CFTP-FCT UNIT 777. A.V. acknowledges support by the ANR project CPV-LFV-LHC NT09-508531.

## References

- [1] G. Aad *et al.* [ATLAS Collaboration], Phys. Lett. B **710** (2012) 49 [arXiv:1202.1408 [hep-ex]].
- [2] S. Chatrchyan *et al.* [CMS Collaboration], Phys. Lett. B **710** (2012) 26 [arXiv:1202.1488 [hep-ex]].
- [3] J. Incandela, for the CMS Collaboration, CERN Seminar, July 4th, 2012.
- [4] F. Gianotti, for the ATLAS Collaboration, CERN Seminar, July 4th, 2012.
- [5] The CDF and D0 Collaborations, FERMILAB-CONF-12-318-E.
- [6] L. J. Hall, D. Pinner and J. T. Ruderman, JHEP **1204** (2012) 131 [arXiv:1112.2703 [hep-ph]].
- [7] H. Baer, V. Barger and A. Mustafayev, Phys. Rev. D **85** (2012) 075010 [arXiv:1112.3017 [hep-ph]].
- [8] J. L. Feng, K. T. Matchev and D. Sanford, Phys. Rev. D **85** (2012) 075007 [arXiv:1112.3021 [hep-ph]].

- [9] S. Heinemeyer, O. Stal and G. Weiglein, Phys. Lett. B **710** (2012) 201 [arXiv:1112.3026 [hep-ph]].
- [10] A. Arbey, M. Battaglia, A. Djouadi, F. Mahmoudi and J. Quevillon, Phys. Lett. B **708** (2012) 162 [arXiv:1112.3028 [hep-ph]].
- [11] A. Arbey, M. Battaglia and F. Mahmoudi, Eur. Phys. J. C **72** (2012) 1906 [arXiv:1112.3032 [hep-ph]].
- [12] P. Draper, P. Meade, M. Reece and D. Shih, Phys. Rev. D **85** (2012) 095007 [arXiv:1112.3068 [hep-ph]].
- [13] T. Moroi, R. Sato and T. T. Yanagida, Phys. Lett. B **709** (2012) 218 [arXiv:1112.3142 [hep-ph]].
- [14] M. Carena, S. Gori, N. R. Shah and C. E. M. Wagner, JHEP **1203** (2012) 014 [arXiv:1112.3336 [hep-ph]].
- [15] U. Ellwanger, JHEP **1203** (2012) 044 [arXiv:1112.3548 [hep-ph]].
- [16] O. Buchmueller, R. Cavanaugh, A. De Roeck, M. J. Dolan, J. R. Ellis, H. Flacher, S. Heinemeyer and G. Isidori *et al.*, arXiv:1112.3564 [hep-ph].
- [17] S. Akula, B. Altunkaynak, D. Feldman, P. Nath and G. Peim, Phys. Rev. D **85** (2012) 075001 [arXiv:1112.3645 [hep-ph]].
- [18] M. Kadastik, K. Kannike, A. Racioppi and M. Raidal, JHEP **1205** (2012) 061 [arXiv:1112.3647 [hep-ph]].
- [19] J. Cao, Z. Heng, D. Li and J. M. Yang, Phys. Lett. B **710** (2012) 665 [arXiv:1112.4391 [hep-ph]].
- [20] A. Arvanitaki and G. Villadoro, JHEP **1202** (2012) 144 [arXiv:1112.4835 [hep-ph]].
- [21] M. Gozdz, arXiv:1201.0875 [hep-ph].
- [22] J. F. Gunion, Y. Jiang and S. Kraml, Phys. Lett. B **710** (2012) 454 [arXiv:1201.0982 [hep-ph]].
- [23] G. G. Ross and K. Schmidt-Hoberg, Nucl. Phys. B **862** (2012) 710 [arXiv:1108.1284 [hep-ph]].
- [24] P. Fileviez Perez, Phys. Lett. B **711** (2012) 353 [arXiv:1201.1501 [hep-ph]].
- [25] N. Karagiannakis, G. Lazarides and C. Pallis, arXiv:1201.2111 [hep-ph].
- [26] S. F. King, M. Muhlleitner and R. Nevzorov, Nucl. Phys. B **860** (2012) 207 [arXiv:1201.2671 [hep-ph]].
- [27] Z. Kang, J. Li and T. Li, arXiv:1201.5305 [hep-ph].
- [28] C. -F. Chang, K. Cheung, Y. -C. Lin and T. -C. Yuan, JHEP **1206** (2012) 128 [arXiv:1202.0054 [hep-ph]].
- [29] L. Aparicio, D. G. Cerdeno and L. E. Ibanez, JHEP **1204** (2012) 126 [arXiv:1202.0822 [hep-ph]].
- [30] L. Roszkowski, E. M. Sessolo and Y. -L. S. Tsai, arXiv:1202.1503 [hep-ph].
- [31] J. Ellis and K. A. Olive, Eur. Phys. J. C **72** (2012) 2005 [arXiv:1202.3262 [hep-ph]].

- [32] H. Baer, V. Barger and A. Mustafayev, JHEP **1205** (2012) 091 [arXiv:1202.4038 [hep-ph]].
- [33] H. Baer, V. Barger, P. Huang and X. Tata, JHEP **1205** (2012) 109 [arXiv:1203.5539 [hep-ph]].
- [34] N. Desai, B. Mukhopadhyaya and S. Niyogi, arXiv:1202.5190 [hep-ph].
- [35] J. -J. Cao, Z. -X. Heng, J. M. Yang, Y. -M. Zhang and J. -Y. Zhu, JHEP **1203** (2012) 086 [arXiv:1202.5821 [hep-ph]].
- [36] L. Maiani, A. D. Polosa and V. Riquer, New J. Phys. **14** (2012) 073029 [arXiv:1202.5998 [hep-ph]].
- [37] T. Cheng, J. Li, T. Li, D. V. Nanopoulos and C. Tong, arXiv:1202.6088 [hep-ph].
- [38] N. D. Christensen, T. Han and S. Su, arXiv:1203.3207 [hep-ph].
- [39] D. A. Vasquez, G. Belanger, C. Boehm, J. Da Silva, P. Richardson and C. Wymant, arXiv:1203.3446 [hep-ph].
- [40] U. Ellwanger and C. Hugonie, arXiv:1203.5048 [hep-ph].
- [41] I. Gogoladze, Q. Shafi and C. S. Un, JHEP **1207** (2012) 055 [arXiv:1203.6082 [hep-ph]].
- [42] M. A. Ajaib, I. Gogoladze, F. Nasir and Q. Shafi, arXiv:1204.2856 [hep-ph].
- [43] F. Brummer, S. Kraml and S. Kulkarni, arXiv:1204.5977 [hep-ph].
- [44] G. G. Ross, K. Schmidt-Hoberg and F. Staub, arXiv:1205.1509 [hep-ph].
- [45] R. Benbrik, M. G. Bock, S. Heinemeyer, O. Stal, G. Weiglein and L. Zeune, arXiv:1207.1096 [hep-ph].
- [46] P. Batra, A. Delgado, D. E. Kaplan and T. M. P. Tait, JHEP **0402** (2004) 043 [hep-ph/0309149].
- [47] A. Maloney, A. Pierce and J. G. Wacker, JHEP **0606** (2006) 034 [hep-ph/0409127].
- [48] M. Hirsch, M. Malinsky, W. Porod, L. Reichert and F. Staub, JHEP **1202**, 084 (2012) [arXiv:1110.3037 [hep-ph]].
- [49] M. Hirsch, W. Porod, L. Reichert and F. Staub, arXiv:1206.3516 [hep-ph].
- [50] H. An, T. Liu and L. -T. Wang, arXiv:1207.2473 [hep-ph].
- [51] L. Randall and M. Reece, arXiv:1206.6540 [hep-ph].
- [52] N. Arkani-Hamed and S. Dimopoulos, JHEP **0506** (2005) 073 [hep-th/0405159].
- [53] S. Dimopoulos and G. F. Giudice, Phys. Lett. B **357** (1995) 573 [hep-ph/9507282].
- [54] D. S. M. Alves, E. Izaguirre and J. G. Wacker, arXiv:1108.3390 [hep-ph].
- [55] M. Dine, A. Kagan and S. Samuel, Phys. Lett. B **243** (1990) 250.
- [56] M. Papucci, J. T. Ruderman and A. Weiler, arXiv:1110.6926 [hep-ph].
- [57] N. Craig, M. McCullough and J. Thaler, JHEP **1206** (2012) 046 [arXiv:1203.1622 [hep-ph]].
- [58] H. Baer, V. Barger, P. Huang, A. Mustafayev and X. Tata, arXiv:1207.3343 [hep-ph].
- [59] L. J. Hall and Y. Nomura, JHEP **1003** (2010) 076 [arXiv:0910.2235 [hep-ph]].
- [60] G. F. Giudice and A. Strumia, Nucl. Phys. B **858** (2012) 63 [arXiv:1108.6077 [hep-ph]].

- [61] N. Polonsky and S. Su, Phys. Lett. B **508** (2001) 103 [hep-ph/0010113].
- [62] A. Brignole, J. A. Casas, J. R. Espinosa and I. Navarro, Nucl. Phys. B **666** (2003) 105 [hep-ph/0301121].
- [63] J. A. Casas, J. R. Espinosa and I. Hidalgo, JHEP **0401** (2004) 008 [hep-ph/0310137].
- [64] M. Dine, N. Seiberg and S. Thomas, Phys. Rev. D **76** (2007) 095004 [arXiv:0707.0005 [hep-ph]].
- [65] E. Ma, Phys. Rev. Lett. **81** (1998) 1171 [hep-ph/9805219].
- [66] P. Minkowski, Phys. Lett. B **67** (1977) 421.
- [67] T. Yanagida, in *KEK lectures*, ed. O. Sawada and A. Sugamoto, KEK, 1979; M Gell-Mann, P Ramond, R. Slansky, in *Supergravity*, ed. P. van Nieuwenhuizen and D. Freedman (North Holland, 1979).
- [68] R. N. Mohapatra and G. Senjanovic, Phys. Rev. Lett. **44** (1980) 912.
- [69] J. Schechter and J. W. F. Valle, Phys. Rev. D **22**, 2227 (1980).
- [70] J. Schechter and J. W. F. Valle, Phys. Rev. D **25** (1982) 774.
- [71] W. Konetschny and W. Kummer, Phys. Lett. B **70**, 433 (1977).
- [72] R. E. Marshak and R. N. Mohapatra, Invited talk given at Orbis Scientiae, Coral Gables, Fla., Jan 14-17, 1980 (Published in Orbis Scientiae 1980:277).
- [73] G. Lazarides, Q. Shafi and C. Wetterich, Nucl. Phys. B **181**, 287 (1981).
- [74] R. N. Mohapatra and G. Senjanovic, Phys. Rev. D **23**, 165 (1981).
- [75] T. P. Cheng and L. -F. Li, Phys. Rev. D **22** (1980) 2860.
- [76] R. Foot, H. Lew, X. G. He and G. C. Joshi, Z. Phys. C **44**, 441 (1989).
- [77] A. Rossi, Phys. Rev. D **66**, 075003 (2002) [arXiv:hep-ph/0207006].
- [78] M. R. Buckley and H. Murayama, Phys. Rev. Lett. **97** (2006) 231801 [hep-ph/0606088].
- [79] J. Adam *et al.* [MEG Collaboration], Phys. Rev. Lett. **107** (2011) 171801 [arXiv:1107.5547 [hep-ex]].
- [80] J. A. Casas and A. Ibarra, Nucl. Phys. B **618**, 171 (2001) [arXiv:hep-ph/0103065].
- [81] F. R. Joaquim, JHEP **1006**, 079 (2010) [arXiv:0912.3427 [hep-ph]].
- [82] For a minimal model see P. Fileviez Perez, Phys. Rev. D **76** (2007) 071701 [arXiv:0705.3589 [hep-ph]].
- [83] Proposal to PSI: “MEG: Search for  $\mu \rightarrow e\gamma$  down to  $10^{-14}$  branching ratio”; Documents and status at <http://meg.web.psi.ch/>. For a status report see, for example: S. Mihara, Nucl. Phys. **A844** (2010) 150C-154C.
- [84] Y. Kuno and Y. Okada, Rev. Mod. Phys. **73**, 151 (2001) [arXiv:hep-ph/9909265].
- [85] M. Raidal, A. van der Schaaf, I. Bigi, M. L. Mangano, Y. K. Semertzidis, S. Abel, S. Albino and S. Antusch *et al.*, Eur. Phys. J. C **57**, 13 (2008) [arXiv:0801.1826 [hep-ph]].
- [86] G. C. Branco, R. G. Felipe and F. R. Joaquim, arXiv:1111.5332 [hep-ph].
- [87] W. Porod, Comput. Phys. Commun. **153**, 275 (2003) [arXiv:hep-ph/0301101].

- [88] W. Porod, F. Staub, [arXiv:1104.1573 [hep-ph]].
- [89] S. P. Martin and M. T. Vaughn, Phys. Rev. D **50** (1994) 2282 [Erratum-ibid. D **78** (2008) 039903] [hep-ph/9311340].
- [90] Y. Yamada, Phys. Rev. D **50** (1994) 3537 [hep-ph/9401241].
- [91] I. Jack and D. R. T. Jones, Phys. Lett. B **333** (1994) 372 [hep-ph/9405233].
- [92] A. Dedes and P. Slavich, Nucl. Phys. B **657** (2003) 333 [hep-ph/0212132].
- [93] D. M. Pierce, J. A. Bagger, K. T. Matchev and R. -j. Zhang, Nucl. Phys. B **491** (1997) 3 [hep-ph/9606211].
- [94] G. Degrandi, P. Slavich and F. Zwirner, Nucl. Phys. B **611** (2001) 403 [hep-ph/0105096].
- [95] A. Brignole, G. Degrandi, P. Slavich and F. Zwirner, Nucl. Phys. B **631** (2002) 195 [hep-ph/0112177].
- [96] A. Brignole, G. Degrandi, P. Slavich and F. Zwirner, Nucl. Phys. B **643** (2002) 79 [hep-ph/0206101].
- [97] A. Dedes, G. Degrandi and P. Slavich, Nucl. Phys. B **672** (2003) 144 [hep-ph/0305127].
- [98] B. C. Allanach, A. Djouadi, J. L. Kneur, W. Porod and P. Slavich, JHEP **0409** (2004) 044 [hep-ph/0406166].
- [99] S. Heinemeyer, W. Hollik and G. Weiglein, Comput. Phys. Commun. **124** (2000) 76 [hep-ph/9812320].
- [100] J. Beringer *et al.* [Particle Data Group Collaboration], Phys. Rev. D **86**, 010001 (2012).
- [101] S. P. Martin, Phys. Rev. D **67**, 095012 (2003) [hep-ph/0211366].
- [102] P. Kant, R. V. Harlander, L. Mihaila and M. Steinhauser, JHEP **1008**, 104 (2010) [arXiv:1005.5709 [hep-ph]].
- [103] S. P. Martin, Phys. Rev. D **75**, 055005 (2007) [hep-ph/0701051].
- [104] J. A. Aguilar-Saavedra, A. Ali, B. C. Allanach, R. L. Arnowitt, H. A. Baer, J. A. Bagger, C. Balazs and V. D. Barger *et al.*, Eur. Phys. J. C **46** (2006) 43 [hep-ph/0511344].
- [105] Y. Okada, M. Yamaguchi and T. Yanagida, Prog. Theor. Phys. **85** (1991) 1.
- [106] J. R. Ellis, G. Ridolfi and F. Zwirner, Phys. Lett. B **257** (1991) 83.
- [107] H. E. Haber and R. Hempfling, Phys. Rev. Lett. **66** (1991) 1815.
- [108] M. S. Carena, J. R. Espinosa, M. Quiros and C. E. M. Wagner, Phys. Lett. B **355** (1995) 209 [hep-ph/9504316].
- [109] M. Tortola, J. W. F. Valle and D. Vanegas, arXiv:1205.4018 [hep-ph].
- [110] G. L. Fogli, E. Lisi, A. Marrone, D. Montanino, A. Palazzo and A. M. Rotunno, arXiv:1205.5254 [hep-ph].
- [111] T. Schwetz, talk at *What is  $\nu$ ?* workshop. Galileo Galilei Institute, Florence, June 25th, 2012.
- [112] G. Aad *et al.* [ATLAS Collaboration], arXiv:1206.1760 [hep-ex].
- [113] S. Chatrchyan *et al.* [CMS Collaboration], arXiv:1207.1898 [hep-ex].

- [114] P. Eerola, f. t. ATLAS, CDF, CMS, D0 and L. collaborations, arXiv:1209.3440 [hep-ex].
- [115] O. Buchmueller, R. Cavanaugh, M. Citron, A. De Roeck, M. J. Dolan, J. R. Ellis, H. Flacher and S. Heinemeyer *et al.*, arXiv:1207.7315 [hep-ph].
- [116] M. Hirsch, S. Kaneko and W. Porod, Phys. Rev. D **78**, 093004 (2008) [arXiv:0806.3361 [hep-ph]].
- [117] J. N. Esteves, S. Kaneko, J. C. Romao, M. Hirsch and W. Porod, Phys. Rev. D **80**, 095003 (2009) [arXiv:0907.5090 [hep-ph]].
- [118] J. N. Esteves, J. C. Romao, M. Hirsch, A. Vicente, W. Porod and F. Staub, JHEP **1012** (2010) 077 [arXiv:1011.0348 [hep-ph]].
- [119] J. N. Esteves, J. C. Romao, M. Hirsch, W. Porod, F. Staub and A. Vicente, JHEP **1201** (2012) 095 [arXiv:1109.6478 [hep-ph]].
- [120] C. Biggio, L. Calibbi, A. Masiero and S. K. Vempati, arXiv:1205.6817 [hep-ph].
- [121] S. Heinemeyer, M. J. Herrero, S. Penaranda and A. M. Rodriguez-Sanchez, JHEP **1105**, 063 (2011) [arXiv:1007.5512 [hep-ph]].
- [122] C. Arbelaez, M. Hirsch and L. Reichert, JHEP **1202** (2012) 112 [arXiv:1112.4771 [hep-ph]].
- [123] S. Antusch, E. Arganda, M. J. Herrero and A. M. Teixeira, JHEP **0611** (2006) 090 [hep-ph/0607263].
- [124] L. Calibbi, A. Faccia, A. Masiero and S. K. Vempati, JHEP **0707** (2007) 012 [hep-ph/0610241].
- [125] M. Hirsch, J. W. F. Valle, W. Porod, J. C. Romao and A. Villanova del Moral, Phys. Rev. D **78** (2008) 013006 [arXiv:0804.4072 [hep-ph]].
- [126] F. R. Joaquim and A. Rossi, Nucl. Phys. B **765**, 71 (2007) [arXiv:hep-ph/0607298].
- [127] F. R. Joaquim and A. Rossi, Phys. Rev. Lett. **97**, 181801 (2006) [arXiv:hep-ph/0604083].
- [128] A. Brignole, F. R. Joaquim and A. Rossi, JHEP **1008** (2010) 133 [arXiv:1007.1942 [hep-ph]].
- [129] C. Biggio and L. Calibbi, JHEP **1010** (2010) 037 [arXiv:1007.3750 [hep-ph]].
- [130] G. Aad *et al.* [ATLAS Collaboration], Phys. Lett. B **716**, 1 (2012) [arXiv:1207.7214 [hep-ex]].
- [131] H. Baer, V. Barger, A. Lessa and X. Tata, arXiv:1207.4846 [hep-ph].
- [132] R. -D. Heuer, arXiv:1202.5860 [physics.acc-ph].
- [133] W. Beenakker, R. Hopker and M. Spira, hep-ph/9611232. For updates see [www.thphys.uni-heidelberg.de/~plehn/](http://www.thphys.uni-heidelberg.de/~plehn/)
- [134] J. N. Esteves, J. C. Romao, M. Hirsch, F. Staub and W. Porod, Phys. Rev. D **83**, 013003 (2011) [arXiv:1010.6000 [hep-ph]].
- [135] G. B. Gelmini and P. Gondolo, Phys. Rev. D **74**, 023510 (2006) [hep-ph/0602230].
- [136] J. N. Esteves, J. C. Romao, A. Villanova del Moral, M. Hirsch, J. W. F. Valle and W. Porod, JHEP **0905**, 003 (2009) [arXiv:0903.1408 [hep-ph]].
- [137] A. J. Buras, L. Calibbi and P. Paradisi, JHEP **1006**, 042 (2010) [arXiv:0912.1309 [hep-ph]].

- [138] A. Abada, A. J. R. Figueiredo, J. C. Romao and A. M. Teixeira, *JHEP* **1108**, 099 (2011) [arXiv:1104.3962 [hep-ph]].